Wiley
Journal of Food Biochemistry
Volume 2025, Article ID 1099383, 19 pages
https://doi.org/10.1155/jfbc/1099383

WILEY

Research Article

Sinomenine Improves Dextran Sodium Sulfate–Induced Chronic Colitis and Associated Memory Disorder in Mice via Gut Microbiota–Mediated SCFAs

Yan Zhou,[1] **Linxiao Wang**,[2] **Jinjin Fu**,[1] **Jie Zhao**,[1] **Dongmei Wang**,[1] **and Liming Tang**[1]

[1]*Digestive Disease Research Center, The Second People's Hospital of Changzhou, the Third Affiliated Hospital of Nanjing Medical University, Changzhou, China*
[2]*Neurology Disease Laboratory, The Second People's Hospital of Changzhou, the Third Affiliated Hospital of Nanjing Medical University, Changzhou, China*

Correspondence should be addressed to Dongmei Wang; dmwang@njmu.edu.cn and Liming Tang; tangliming@njmu.edu.cn

Received 14 October 2024; Revised 13 November 2025; Accepted 15 November 2025

Academic Editor: Xuelin Zhou

Copyright © 2025 Yan Zhou et al. Journal of Food Biochemistry published by John Wiley & Sons Ltd. This is an open access article under the terms of the Creative Commons Attribution License, which permits use, distribution and reproduction in any medium, provided the original work is properly cited.

Sinomenine is extracted from the root of Chinese herb QingTeng (*Sinomenium acutum* (Thunb.) Rehd. Et wils.), which is extensively utilized by traditional medical practitioners for its anti-inflammatory and immunoregulatory properties in China for decades. The aim of this study was to assess the effects and potential mechanisms of sinomenine in alleviating dextran sodium sulfate (DSS)–induced chronic colitis and memory disorder in mice. A mouse chronic colitis model was established by 2.5% DSS, and sinomenine treatment was oral administration. It showed that sinomenine inhibited weight loss, colon shortening, proinflammatory cytokine production, and intestinal barrier injury in the colon. Sinomenine improved inflammatory bowel diseases (IBD) and accompanying memory disorders with downregulated expressions of proinflammatory cytokines and neuronal apoptosis; upregulated expressions of brain-derived neurotrophic factor (BDNF) and ZO-1 in the hippocampus. Additionally, our findings indicated that sinomenine altered the composition of various gut microbiota, leading to an increase in Bacteroidetes and Firmicutes at the phylum level, and *Rikenella* at the genus level. Moreover, sinomenine ameliorated the SCFA content in DSS-induced mice both in serum and feces. The findings demonstrated that sinomenine ameliorated DSS-induced chronic colitis and accompanying memory disorders.

Keywords: colitis; gut microbiota; intestinal barrier; neuroinflammation; SCFAs; sinomenine

1. Introduction

Ulcerative colitis (UC) and Crohn's disease (CD) are two common forms of IBD [1]. Patients with IBD often experience weight loss, frequent diarrhea, stomach pain, and bleeding from the rectum, which can advance to passing blood in the stool [2]. Chronic symptoms of human IBD are characterized by a state of recurring flare-ups and remissions. Because of the variable progression of the illness, individuals with IBD frequently experience symptoms of common mental disorders [3, 4]. In contemporary society, psychological disorders linked to colitis have emerged as a significant threat to human well-being. Unfortunately, there is no effective treatment for this condition [5].

The brain can interact with the digestive system through a sophisticated gut–brain connection. The gut mucosal barrier and the blood–brain barrier (BBB) are crucial for preserving intestinal and central equilibrium, as well as immune tolerance [6, 7]. Colitis triggers adverse behaviors via the microbiota–gut–brain axis, leading to immune system irregularities, disruptions in gut microbiota balance, and compromised barrier function. Enhanced gut permeability in individuals with long-term UC allows inflammatory agents to access the brain, compromising the

blood–brain barrier [8, 9]. Inflammation in the intestines may lead to neuro-inflammation, and the interplay between gut and brain inflammation can worsen intestinal harm [10]. Interactions between gut microbes and their host could play a role in the two-way communication between the digestive system and the brain, particularly noted in the context of IBD [11].

Sinomenine (SIN), an alkaloid originated from the traditional Chinese medicinal plant named *Sinomenium acutum*, exhibits strong anti-inflammatory and immune-modulating properties, along with sedative and pain-relieving effects, and is extensively utilized in China for arthritis treatment [12, 13]. The hydrochloride form of SIN, named ZhengQing FengTongNing (ZQFTN) tablets, has been listed in the Chinese Pharmacopeia for years [14, 15]. SIN had low absorption into the bloodstream, yet it was able to alter gut microbiota to help prevent diseases linked to chronic inflammation [16]. Our previous studies found that SIN could effectively improve DSS-induced acute UC and regulate gut microbiota [17, 18]. Nevertheless, the impacts and underlying processes of SIN in DSS-induced chronic colitis and cognitive impairments are still not well understood.

Therefore, the intervention effects and mechanisms of SIN in DSS-induced chronic colitis mouse model were explored in this study. Salicylazosulfapyridine (SASP), a medication for treating IBD in clinical settings, served as the positive control drug. This research explored gut homeostasis, focusing on inflammation, barrier function, and microbiota, as well as the neuroprotective impacts, including inflammation and barrier integrity. Furthermore, the fundamental processes, particularly the essential gut microbes and significant microbial signaling metabolites linked to neuroprotective effects of SIN, will be investigated using 16S rRNA–based microbiota analysis and metabolomics profiling.

2. Materials and Methods

2.1. Reagents and Chemicals. Sinomenine hydrochloride (Cat.no. S27281) was acquired from Shanghai Yuanye Bio-Technology Co., Ltd. (Shanghai, China). The Lot. identifier is C11M11Y112638, with a purity exceeding 99%. MP Biomedical (Aurora, OH, USA) supplied DSS (Cat.no. 0216011080), with a molecular weight range of 36,000–50,000 Da. Every other chemical utilized was of analytical quality.

2.2. Animals and Chronic Colitis Model Establishment. The experimental protocols were conducted in accordance with the European Community guidelines (86/609/EEC) [19]. Animal ethics approval was obtained from the Nanjing Medical University Animal Care and Use Committee. The study utilized 8-week-old female C57BL/6J mice, each weighing between 18 and 22 g, supplied by Changzhou Cavens Laboratory Animal Co., Ltd. The animal certificate number is SCXK[SU]2021-0013. We chose the female mice because earlier studies showed that males were more vulnerable and had a greater death rate when subjected to repeated DSS treatments [20, 21]. These mice were housed in a regulated setting with a temperature of 25 C ± 2°C, humidity levels of 60% ± 5%, and exposed to a 12-h light and dark cycle.

After a week of adaptive feeding, 40 mice were randomly divided into four groups. A persistent UC model was created by giving three rounds of 2.5% DSS solution in drinking water; 400 mg/kg SASP or 100 mg/kg SIN was administered every day by oral gavage during the indicated period. Every cycle consisted of DSS for 5 days followed by 10 days of normal drinking water. Figure 1(a) illustrates the particular methods of administration. The DSS + SIN group was given SIN (100 mg/kg); the dosage selection was based on the results of our previous studies [17, 18], which showed that 100 mg/kg SIN could significantly improve DSS-induced colitis in mice. Therefore, 100 mg/kg SIN was selected for subsequent analysis in this research.

2.3. Contextual Fear Conditioning Test. Behavioral analyses were performed in a blinded manner. This test was performed 5 days after cessation of every round DSS drinking. In brief, round 1, 2, and 3 CF tests were conducted on Days 10, 25, and 40, respectively. In the training period, mice were introduced to the conditioning chamber for 5 min to get accustomed. Subsequently, they experienced 30 s of auditory stimulation (4,000 Hz, 100 dB), then received three foot shocks (0.6 mA, lasting 2 s each, with a 1-min interval). Behavioral tests were administered 1 h (short term) and 24 h (long term) after the training phase. During the retrieval test, after adapting to the new environment for 3 min, the mice were given 30 s of sound stimulation (4,000 Hz, 100 dB). Once every mouse finished the test, we meticulously clean the container to eliminate any lingering scent that could skew the experimental outcomes. The proportion of time the animals remained motionless, except for breathing, was utilized as an indicator of contextual fear. The degree of freezing is represented as a percentage of the entire scoring duration. During this experiment, the machine automatically logged the proportion of time spent in a frozen state.

2.4. Morphological and Histopathological Examination. The mice were monitored and their body weights were recorded every 2–3 days. After sacrificed, the entire colon was extracted and its length was measured. The colon tissue was subsequently split into three parts, with the smallest segment immersed in 10% neutral buffered formalin (NBF) for further hematoxylin and eosin (H&E) and immunohistochemical staining. The leftover portions were kept at −80°C for future examination. In addition, the spleens of mice were weighed.

2.5. Brain and Hippocampi Sample Preparation. Mice were fully anesthetized by drop jar method using isoflurane, and then the blood was collected from retro-orbital plexus according to UCSF-IACUC guidelines (https://iacuc.ucsf.edu/guidelines). Later, five mice from each cohort

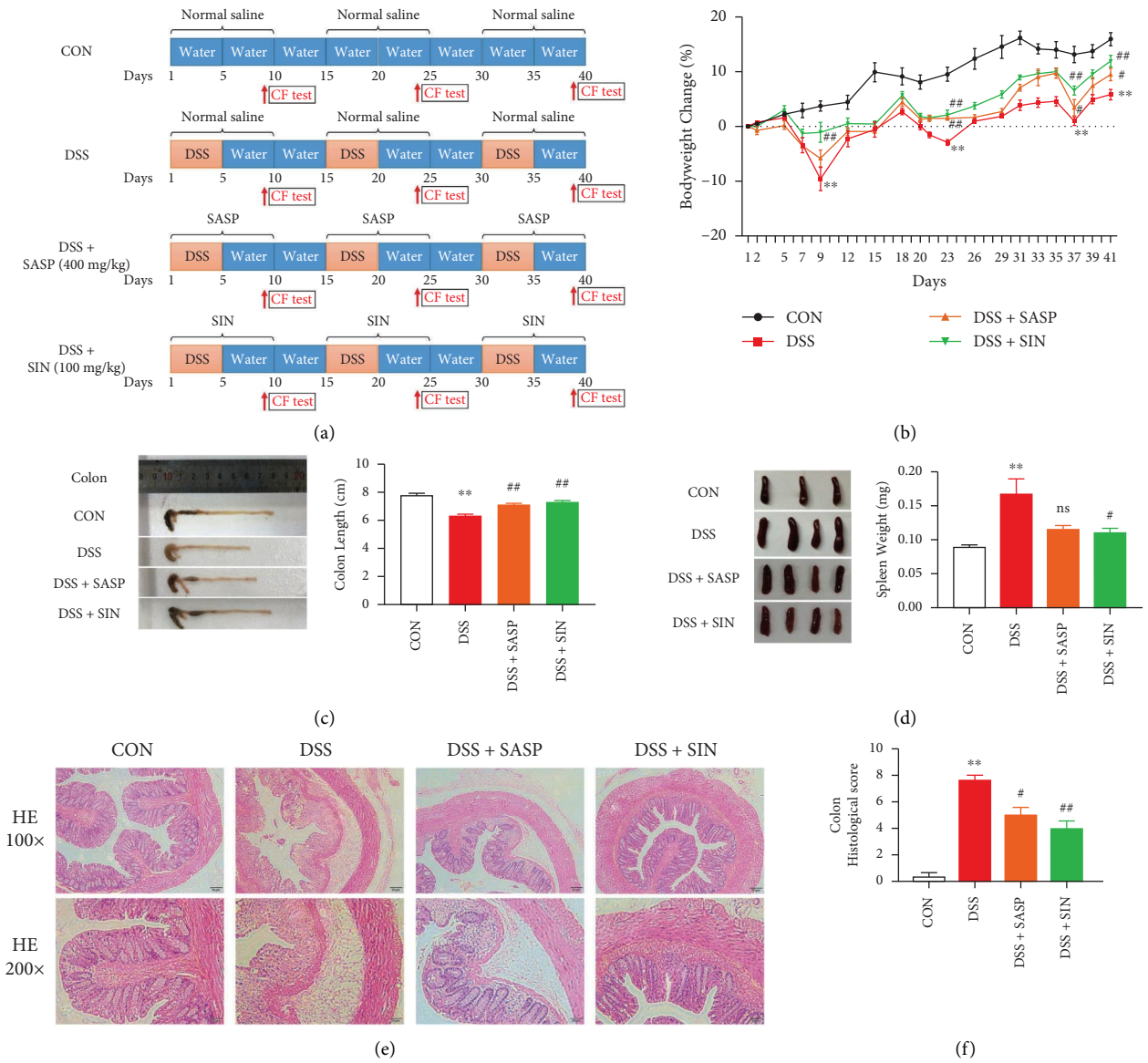


Figure 1: Sinomenine improved DSS-induced chronic colitis. (a) List of designed animal experiments. (b) Changes in body weight of mice. (c) Colon length. (d) Spleen weight. (e) Representative HE staining images of the colon sections. (f) Colon histological score. Data are presented as the mean ± SEM, $n = 3$–9. $^{*}p < 0.05$ and $^{**}p < 0.01$ compared with the control group (CON), $^{\#}p < 0.05$ and $^{\#\#}p < 0.01$ compared with the DSS group (DSS), ns, no significant difference.

underwent transcardial perfusion with 10% NBF, and their whole brains were preserved in 10% NBF for later IHC. The brains of the remaining mice in each group were harvested and preserved at −80°C for subsequent examination.

2.6. Immunohistochemistry (IHC). Adhering to the IHC guidelines, the colon and hippocampal tissues of mice were treated with ZO-1 (Cat.no. GB111402, Servicebio Biotechnology, China) and Occludin (Cat.no. GB111401, Servicebio Biotechnology, China) primary antibodies. The colon slices were incubated with a specific MUC2 primary antibody (Cat.no. GB11344, Servicebio Biotechnology, China) for immunostaining. The hippocampal slices from the mice were treated with a specific brain-derived neurotrophic factor (BDNF) primary antibody (Cat.no. GB11559, Servicebio Biotechnology, China) for immunostaining.

2.7. Nissl Staining. Dewaxed and hydrated paraffin sections were prepared according to standard procedures. Nissl solution (Cat.no. G1036, Servicebio Biotechnology, China) was used to stain for 5 min at room temperature. After that, the segments were rinsed with purified water to remove the dye, dried with a series of alcohol concentrations, cleared with xylene, and finally sealed with neutral resin to finalize the staining process. A light microscope was used to examine and capture images of the hippocampus in a coronal slice.

2.8. TUNEL Assay. Hippocampal apoptosis was evaluated by TUNEL assay. DAB (SA-HRP) Tunel Cell Apoptosis Detection Kit (Cat.no. G1507, Servicebio Biotechnology, China) was performed on brain sections according to the manufacturer's instructions. A light microscope was employed to identify neuronal apoptosis in the hippocampus.

2.9. RNA Isolation and Quantitative Real-Time PCR. Real-time quantitative reverse transcription polymerase chain reaction (RT-qPCR) was employed to measure the mRNA levels of inflammatory cytokines (IL-1β, IL-6, TNF-α) and BDNF. Total RNA was extracted from mouse colons and brains using the RNAsimple Total RNA kit (Cat.no. DP419, TIANGEN, China) according to the provided instructions. cDNA was produced from the extracted RNA with the HiScript II Q RT SuperMix for qPCR (+gDNA wiper) (Cat.no.R223, Vazyme, China). The RT-PCR procedure involved 15 min at 50°C, followed by 5 s at 85°C, and finally cooling down to 4°C. Real-time PCR was conducted using AceQ qPCR SYBR Green Master Mix (Cat.no. Q131-02, Vazyme, China) and the ABI 7500 system. The reaction was conducted at 95°C for 5 min, then cycled 40 times at 95°C for 10 s and 60°C for 30 s. The mRNA levels of each target gene were adjusted relative to GAPDH. The primers mentioned earlier are displayed in Table 1. Gene expression fold changes were determined through the $2^{-(\Delta\Delta Ct)}$ technique as described by Livak and Schmittgen in 2001 [22].

2.10. Protein Extraction and Western Blot Analysis. Using a Protein Extraction Kit (Cat.no.P0013, Beyotime, China) and a Protease and Phosphatase Inhibitor Cocktail (Cat.no. 1045, Beyotime, China), proteins were extracted from the colons and brains of mice following the manufacturer's instructions. Following quantification, the aforementioned protein extracts were combined with 5× SDS-PAGE sample loading buffer (Cat.no. P0015, Beyotime, China) and heated for 10 min. After 10% SDS-PAGE (Cat.no. G2043, Servicebio, China), the protein samples (30 μg/lane) were separated and transferred onto PVDF membranes (Cat.no. ISEQ00010, MerkMillipore, MA, USA). Subsequently, the PVDF membranes were incubated for 30 min to block them with a protein-free quick blocking solution (Cat.no. G2052, Servicebio, China) at room temperature. The PVDF membranes were incubated with the specific primary antibodies ZO-1 (Cat.no. GB111402 Servicebio, China), Occludin (Cat.no. GB111401, Servicebio, China), BDNF (Cat.no. GB11559, Servicebio, China), and β-actin (Cat.no. TA7018S, Abmart, China), all diluted 1:1000, at 4°C overnight, followed by washing with 1× TBST buffer (Cat.no.G2150, Servicebio, China). After that, the membranes were incubated with a secondary antibody (Cat.no.GB23303, Servicebio, China) diluted 1:5000 for 1 h at room temperature. Proteins in the PVDF membranes were imaged using Enhanced Chemiluminescent Kit (Cat.no. M0103, KerMey, China). ImageJ software was utilized to measure the protein immunoblots.

Table 1: Primer sequences for reverse transcription-quantitative polymerase chain reaction.

	Gene	Sequences (5′-3′)
Mouse	TNF-α F	CACAGAAAGCATGATCCGCGACGT
	TNF-α R	CGGCAGAGAGGAGGTTGACTTTCT
	IL-1β F	GCAACTGTTCCTGAACTCAACT
	IL-1β R	ATCTTTTGGGGTCCGTCAACT
	IL-6 F	GACAACCACGGCCTTCCCTA
	IL-6 R	GGTACTCCAGAAGACCAGAGGA
	BDNF F	TCATACTTCGGTTGCATGAAGG
	BDNF R	ACACCTGGGTAGGCCAAGTT
	GAPDH F	CATGGCCTTCCGTGTTC
	GAPDH R	CCTGGTCCTCAGTGTAGC

2.11. 16S rRNA Gene Sequencing Analysis. The fecal contents from the cecum were frozen rapidly and stored at a temperature of −80°C for analysis. 16S rRNA amplicon sequencing was conducted by Applied Protein Technology Company (Zhejiang, China). In brief, the total genomic DNA was extracted from the fecal sample using either the CTAB or SDS technique, and its concentration was measured with a NanoDrop spectrophotometer. DNA purity was monitored on 1% agarose gels. According to the concentration, DNA was later diluted to 1 ng/μL using sterile water. Primer: 16S V3-V4: 341F-806R. 16S rRNA genes were amplified and the specific primer was used with the barcode. All PCR reactions were carried out in 30-μL reactions with 15 μL of PhusionHigh-Fidelity PCR Master Mix (New England Biolabs); 0.2 μM of forward and reverse primers, and about 10-ng template DNA. Mix same volume of 1X loading buffer (contained SYB green) with PCR products and operate electrophoresis on 2% agarose gel for detection. Samples with bright main strip between 400 and 450 bp were chosen for further experiments. PCR products were mixed in equidensity ratios. Then, mixture PCR products were purified with AxyPrepDNA Gel Extraction Kit (AXYGEN). Sequencing libraries were generated using NEB NextUltraDNA Library Prep Kit for Illumina (NEB, USA) following the manufacturer's recommendations, and index codes were added. The library quality was assessed on the Qubit@ 2.0 Fluorometer (Thermo Scientific) and Agilent Bioanalyzer 2100 system. At last, the library was sequenced on an Illumina Miseq/HiSeq2500 platform and 250 bp/300 bp paired-end reads were generated.

To gauge α-diversity, the ACE, Chao1, and Shannon indices were calculated with *t* test. The Weighted Unifrac distance or Unweighted Unifrac distance was calculated to measure the phylogenetic β-diversity using QIIME. The results were shown through boxplots, and the *t*-test was also used to analyze whether there were significant differences between groups. Nonmetric multi-dimensional scaling (NMDS) was performed to show the similarities or differences in the composition of the sample community. KEGG functional predictive analysis is an effective way to study the changes in metabolic functions of community samples to adapt to environmental changes. PICRUSt software was used to compare species composition information obtained from 16S sequencing data, then the functional gene

composition in the samples can be inferred. To confirm differences in the abundances of individual taxonomy between the two groups, STAMP software was utilized with Welch's *t*-test.

2.12. Detection of Specific Short-Chain Fatty Acids (SCFAs). The targeted SCFAs determination was conducted by Applied Protein Technology Company (Zhejiang, China). In brief, the samples of mice serum were thawed on ice, and 100-μL samples were taken into 2-mL tubes. Then, 900 μL of 0.5% phosphoric acid was added to the suspension, followed by shaking, mixing, and centrifugation. Next, 800 μL of the supernatant was taken, and an equal volume of ethyl acetate was added for extraction A volume of 600 μL from the upper organic layer was collected, and 4-methylvaleric acid was introduced to achieve a final concentration of 500 μM as an internal standard. This mixture was then transferred to the sample vial for GC-MS analysis.

The feces samples were thawed at 4°C, and 100 mg of each sample was mixed with 50 μL of water with 20% phosphoric acid and 500 μL of isopropyl ether with 500-μM 4-methyl valeric acid (IS), adequately vortex. The mixture was centrifuged for 20 min (14,000rcf, 4°C), then the supernatants were collected for GC-MS analysis. The injection volume was 1 μL, and the shutter ratio was 10:1. The specimens were analyzed using an Agilent DB-WAX capillary column in a gas chromatography setup. Starting at 90°C, the temperature was increased to 120°C at a rate of 10°C per minute, then to 150°C at 5°C per minute, and finally to 250°C at 25°C per minute, where it was held for 2 min. The helium gas flows at a rate of 1.0 mL per minute. To assess the system's stability and consistency, a quality control sample was periodically placed among the experimental samples in the queue. An Agilent 7890 A/5975C gas-mass spectrometer (Agilent, USA) was used for MSElectron impact ionization source [3], utilizing both full-scan and SIM scan modes, with an electron energy of 70 eV. MSD ChemStation software was utilized to obtain the retention time and peak area from the chromatogram. The levels of SCFAs in the sample were determined using a standard curve.

2.13. Statistical Analysis. For this research, we utilized GraphPad Prism 8 to perform the statistical analysis of the experimental results. The results were presented as mean ± SEM. The data was analyzed using one-way ANOVA, followed by Bonferroni's multiple comparison test. A *P*-value less than 0.05 indicates that the variation in variables is statistically meaningful.

3. Results

3.1. SIN Improved DSS-Induced Chronic Colitis in Mice. To investigate the impact of SIN on DSS-triggered chronic colitis, the bodyweight, colon condition, and spleen index of each mouse were monitored. DSS dramatically decreased the bodyweight, while SASP (positive-drug) and SIN treatment improved it (Figure 1(b)), which indicated the alleviative effect of SASP and SIN in loss of weight in colitis. Furthermore, DSS caused harm to the colon tissue, leading to a significant reduction in colon length compared to the control group. However, treatment with SASP and SIN notably increased the colon length ratio in comparison to the DSS model group (Figure 1(c)), which indicated their protective effect against colon shortening. Pathological alterations in colonic tissue were observed after H&E staining. As demonstrated through H&E staining (Figure 1(e)), the control group of mice exhibited a typical colon architecture with intact intestinal glands, whereas DSS treatment caused significant disruption to the epithelial lining and extensive damage to the majority of the intestinal glands, resulting in a more pronounced separation between tissues than observed in the control mice. Nevertheless, the addition of SASP and SIN notably alleviated these conditions. Colon histological analysis also showed that SASP and SIN could repair colon tissue injury caused by DSS (Figure 1(f)).

Normally, the ratio of splenic weight to body weight remains constant. Measurement of splenic weight is one of the major methods to assess host immunity status [23, 24]. Additionally, we evaluated how SIN affects the spleen. Our data indicated that DSS significantly increased the spleen weight, while SASP and SIN treatment seemed alter the swelling of the spleen (Figure 1(d)), which suggested that supplementation of SASP or SIN could improve the immunity during colitis. Taken together, these findings demonstrate that SIN can effectively relieve the symptoms of chronic colitis in a murine model.

3.2. SIN Alleviated Hippocampal Damage Following DSS-Induced Chronic Colitis. Hippocampal neurons serve as the neural foundation of learning and memory, and their apoptosis leads to reduced function such as fear regulation and memory [25]. Nissl staining, frequently employed to determine neuron viability in brain tissue, was utilized to evaluate morphological alterations in the hippocampus [26]. In contrast to the control group, DSS caused a decrease in hippocampal neurons, irregular Nissl bodies, disrupted organization, and marked nuclear abnormalities (indicated by the red arrow) (Figure 2(a)). Nonetheless, SIN therapy enhanced the structure of mouse neurons relative to the DSS group. There is no significant change between DSS + SASP and DSS group (Figure 2(b)). It suggested that chronic colitis remarkably impacts the neuron's morphology and quantity, while SIN demonstrates neuroprotection effect in mice.

Following the Nissl staining outcomes, we delved deeper into the impact of SIN on the fear conditioning assessment (Figure 2(c)). As shown in Figure 2(d), freezing time (%) did not alter significantly among different groups in short terms. In long terms, mice in DSS group presented a significant reduction in freezing behavior compared to controls in R3-long term (from 51.675% to 24.575%, $p = 0.011$), while the DSS + SIN treatment improved this reduction (the freezing time raised to 45%, $p = 0.044$); SASP supplementation did not have such effect (the freezing time raised to 32.125%, but there was no statistical difference) (Figure 2(e), blue rectangle marked). In addition, there were no statistical difference in movement distance and mean velocity of motion

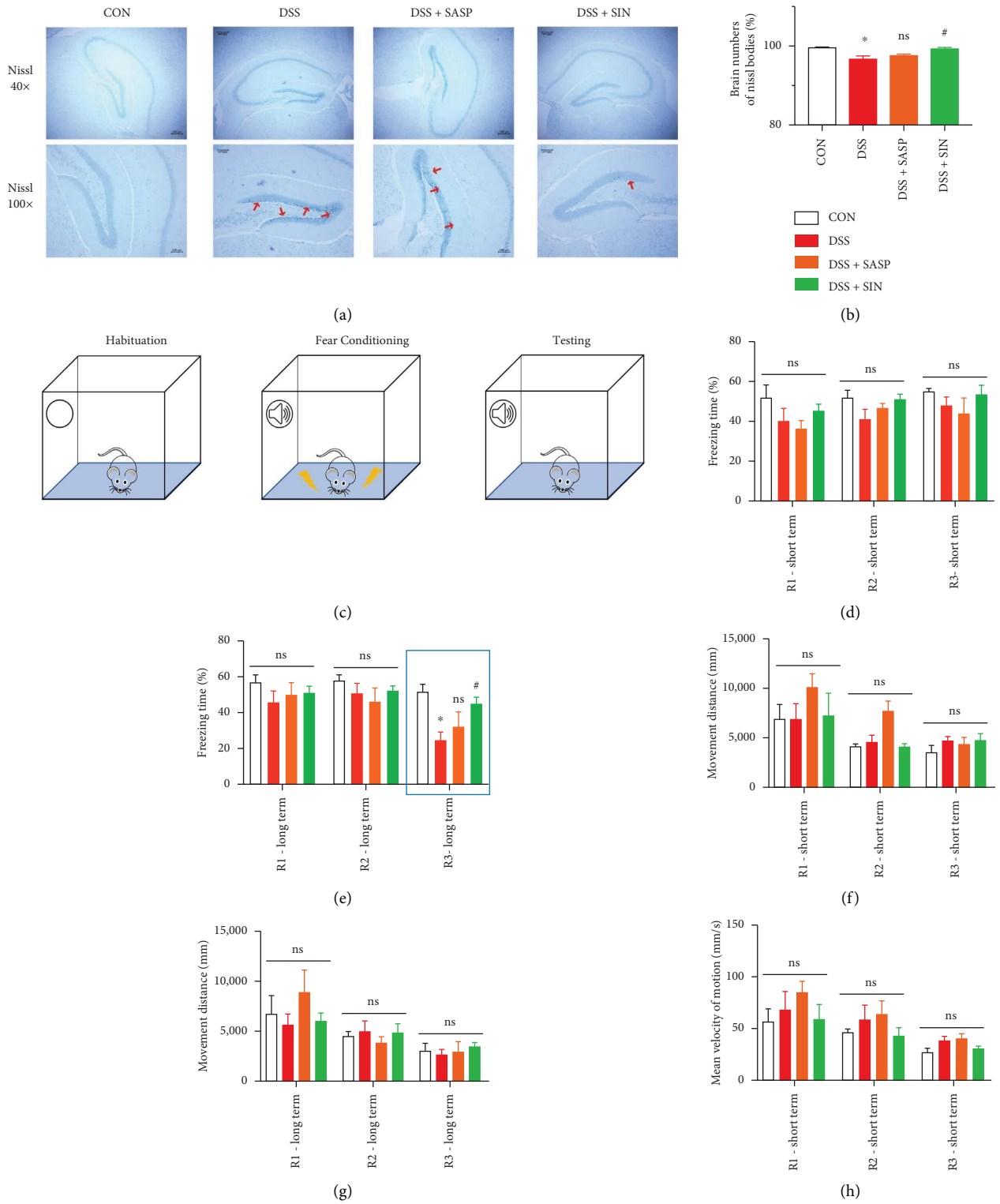


Figure 2: Continued.

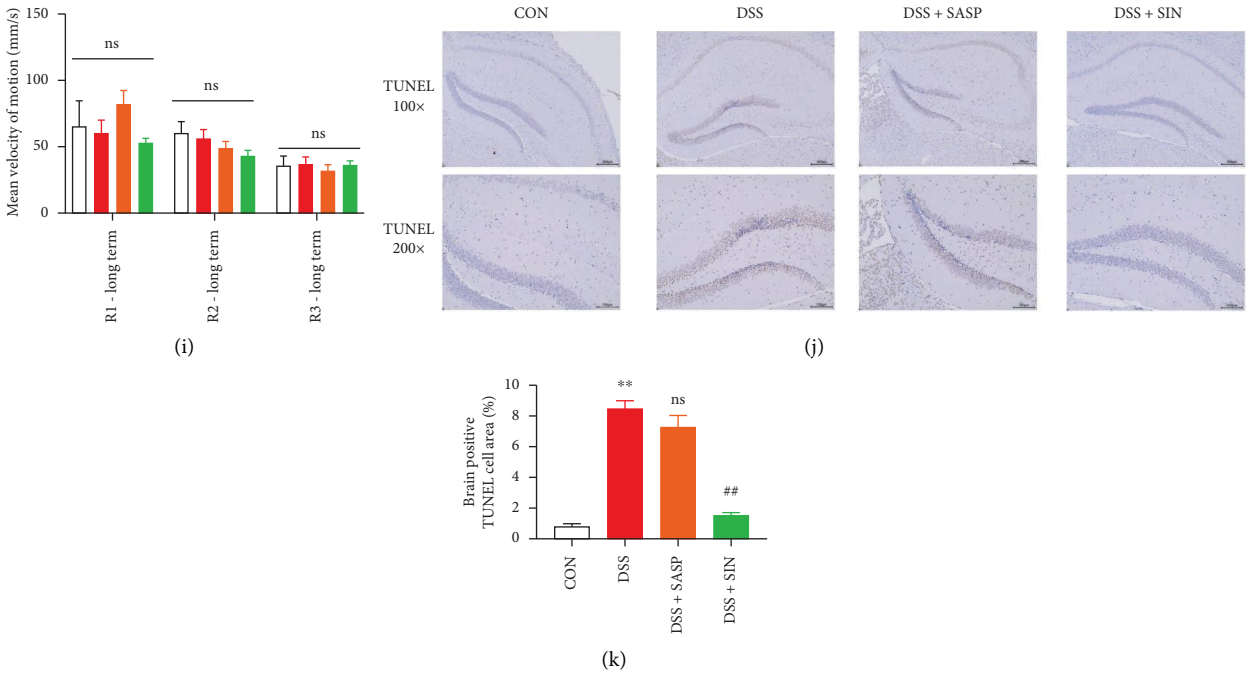


Figure 2: SIN alleviated hippocampal damage following DSS-induced chronic colitis. (a) Nissl staining of brains in the hippocampus. (b) Statistical data of (a). (c) Diagram of contextual fear conditioning test. In contextual fear conditioning assessment, (d) freezing time, (f) movement distance, and (h) mean velocity of motion in short term were recorded; (e) freezing time, (g) movement distance, and (i) mean velocity of motion in long term were calculated. (j) TUNEL staining of brains in the hippocampus. (k) Statistical data of (j). Data are presented as the mean ± SEM, $n = 3$–9. $^{*}p < 0.05$ and $^{**}p < 0.01$ compared with CON; $^{\#}p < 0.05$ and $^{\#\#}p < 0.01$ compared with DSS; ns, no significant difference.

among different treatments, whether it was in short or long term (Figures 2(f), 2(g), 2(h), 2(i)).

Hippocampus is involved in reconsolidation and extinction of contextual fear memory [27]. We then detected TUNEL staining of mouse brain. TUNEL staining indicated that DSS exposure induced cell death in the hippocampus, whereas SIN treatment mitigated this outcome (Figures 2(j), 2(k)). These findings indicated that SIN might effectively counteract the long-term memory impairment induced by DSS in chronic colitis.

3.3. SIN Reversed DSS-Induced Intestinal Inflammation and Barrier Integrity. The intestinal mucosal acts as a biological shield, stopping dangerous substances from penetrating the bloodstream and tissues [28]. ZO-1 and Occludin are crucial proteins, which form the essential elements of tight junction (TJ) barrier. We further assessed the impact of SIN on inflammatory cytokines in colon tissues. The DSS group of mice exhibited elevated TNF-α, IL-6, and IL-1β levels compared to the control group, which significantly decreased following SASP and SIN treatments (Figures 3(a), 3(b), and 3(c)). Given the damage to epithelial cells, western blotting was used to examine TJ proteins in the colon, such as ZO-1 and Occludin. In the DSS group, ZO-1 and Occludin levels dropped from 1 to 0.45 and 0.44, respectively. However, in the DSS + SIN treatment group, these levels rose to 0.70 and 0.73, and in the DSS + SASP treatment group, they increased to 0.47 and 0.77, respectively (Figures 3(d), 3(e), 3(f)). The expression of ZO-1 and Occludin in colon tissues was also evaluated by IHC. As shown in Figures 3(g) and 3(h), the expressions of ZO-1 and Occludin were notably reduced in the colon tissues of DSS group, compared with that in the CON group. However, both DSS + SASP and DSS + SIN treatments obviously increased the levels of ZO-1 and Occludin. The quantitative results of IHC are shown in Figures 3(i) and 3(j). In addition, we detected the expression of mucin-2 (MUC-2) protein, which is synthesized and secreted by goblet cells from the mucus layer. As shown in Figure 3(k), MUC2 was notably reduced in the colon tissues of DSS group, compared to the CON group, while DSS + SASP and DSS + SIN treatments increased the levels of MUC2. The quantitative results of IHC are shown in Figure 3(l). These findings indicated that intestinal barriers were compromised following DSS exposure, but treatment with SASP or SIN could partially mitigate the damage.

3.4. SIN Protected Against DSS-Induced Imbalance of Neuroinflammation and ZO-1, BDNF Expressions. We detected the mRNA levels of proinflammatory factors in mouse brain tissue. Mice administered DSS showed elevated concentrations of TNF-α, IL-6, and IL-1β compared to the control group (Figures 4(a), 4(b), and 4(c)). BBB primarily consists of epithelial cells linked by TJ proteins or other supportive structures [29]. In the chronic UC mice, a reduction in ZO-1 and Occludin protein levels was observed in brain tissues,

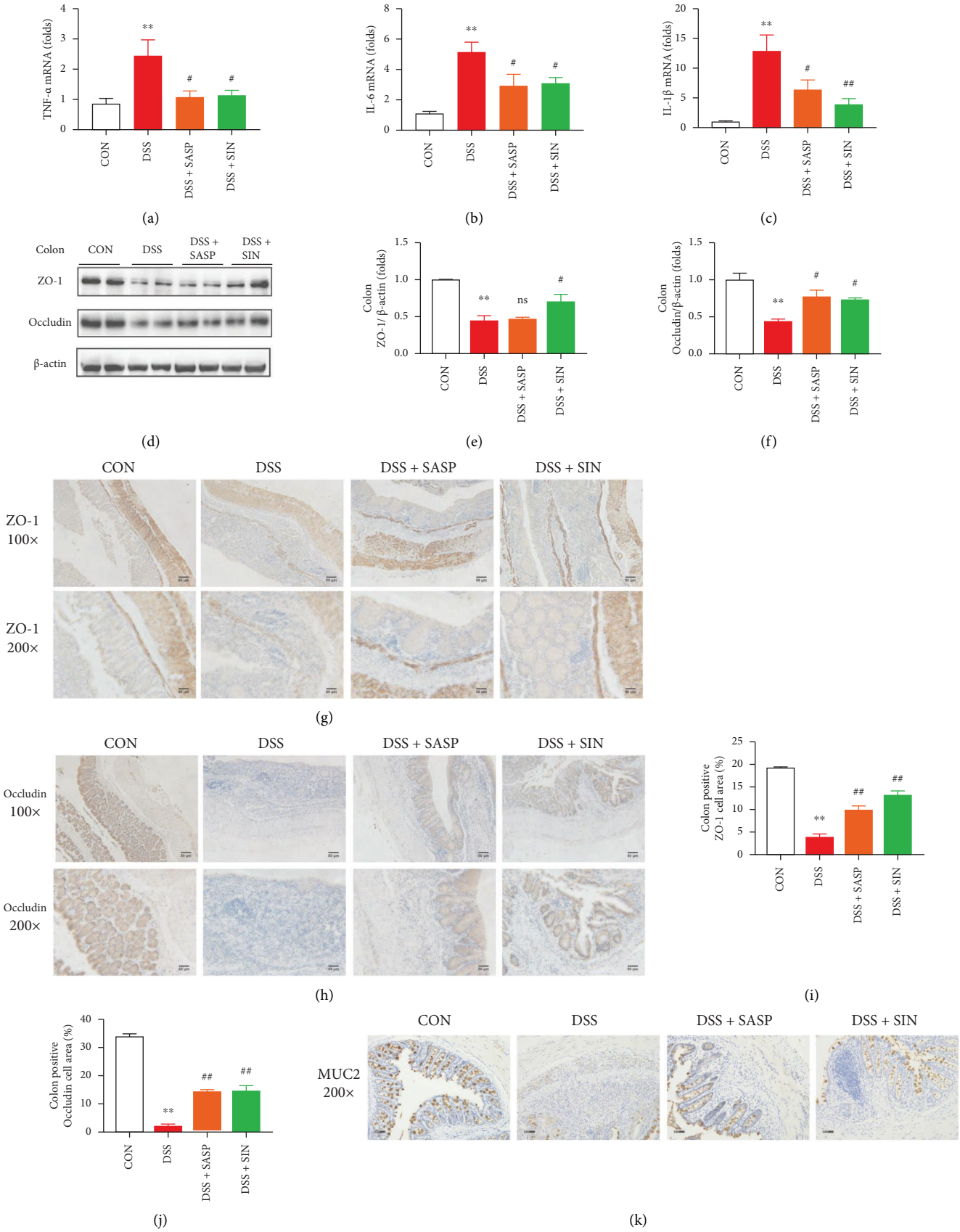


Figure 3: Continued.

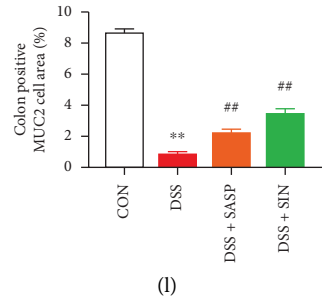


FIGURE 3: SIN reversed DSS-induced intestinal inflammation and barrier integrity. The relative mRNA level of (a) TNF-α, (b) IL-6, and (c) IL-1β in the colon tissues. (d) Western blot analysis of ZO-1 and Occludin in the colon tissues. (e, f) Densitometry analysis of (d). Representative immunohistochemical micrographs of (g) ZO-1 and (h) Occludin protein in the colon. (i) Statistical data of (g). (j) Statistical data of (h). (k) MUC2 immunohistochemical micrographs. (l) Statistical data of (k). Data are presented as the mean ± SEM, $n = 3–6$. $^{*}p < 0.05$ and $^{**}p < 0.01$ compared with CON, $^{\#}p < 0.05$ and $^{\#\#}p < 0.01$ compared with DSS, ns, no significant difference.

which could be reversed by SASP and SIN treatment, although the change in Occludin was not statistically significant (Figures 4(d), 4(e), and 4(f)). The IHC staining results consistently indicated that SIN could elevate the levels of ZO-1 and Occludin (Figures 4(g), 4(h), 4(i), and 4(j)).

BDNF is extensively found throughout the brain and is crucial for supporting the development and specialization of neurons [30]. Mice treated with DSS showed a notable decrease in BDNF levels, while were significantly recovered following SIN therapy (Figures 4(k), 4(l), and 4(m)). BDNF has emerged as a key regulator of cognitive performance and brain health in distinct brain regions, including hippocampus and cortex [31]. The IHC findings indicated a decrease in BDNF levels in the cortical and hippocampal regions of mice treated with DSS, whereas SIN notably counteracted this effect (Figures 4(n), 4(o), 4(p), and 4(q)). Nevertheless, SASP, the clinical medicine of colitis, did not influence these cognitive impairments. It indicated that SIN showed neuronal protection and cognitive function by enhancing the expression of BDNF. Taken together, these results prompted that SIN successfully reduced neuroinflammation, maintained BBB integrity, and elevated BDNF levels to safeguard neurons.

3.5. SIN Impacted the Irregular Gut Microbiota Composition in DSS-Induced Chronic Colitis Mice. Disruptions in gut bacteria and unusual metabolic byproducts can influence the gut–brain axis [32]. To explore the impact of SIN on the altered gut microbiota caused by DSS, the 16S rRNA genes in the cecal contents of mice were sequenced. To assess the richness and variety of gut microbiota, analyses of α-diversity and β-diversity were conducted on fecal samples. The α-diversity assessment, encompassing Shannon, ACE, and Chao1 indices, revealed that DSS + SIN treatment enhanced the microbiota diversity in mice with DSS-induced chronic UC (Figures 5(a), 5(b), and 5(c)), indicating the restoration of gut microbiota. The results of β-diversity based on Weighted Unifrac and Unweighted Unifrac Beta distance are shown in Figures 5(d) and 5(e). NMDS revealed a significant difference in the bacterial community composition between the DSS and CON groups. In contrast, the DSS + SIN group showed a closer resemblance to the CON group than to the DSS group (Figure 5(f)).

Next, we analyzed the species' distribution across various tiers. The stacked bar chart illustrated the variations in relative abundance at the phylum, class, and genus levels. The dominant phyla were mainly Bacteroidetes and Firmicutes (Figure 5(g)). Compared to the CON group, the DSS group exhibited reduced levels of Bacteroidetes and Firmicutes, whereas the DSS + SIN treatment elevated the abundance of these major phyla (Figures 5(h) and 5(i)). In mice with DSS-induced chronic colitis, there was a reduced presence of Bacteroidia and Clostridia at the class level. Nevertheless, SIN involvement led to an increase in the quantity of this category (Figures 5(j), 5(k), 5(l)). At the genus level, DSS treatment dramatically reduced the relative abundance of *Ruminococcaceae UCG-014* and *Alloprevotella*, while DSS + SIN treatment showed a slight rise in *Alloprevotella* (Figures 5(m), 5(n), 5(o)). Since there were no statistical differences between DSS and DSS + SIN groups in the relative abundance of gut microbiota composition, Statistical Analysis of Metagenomic Profiles (STAMP) was applied to explore the key different gut microbiota. As shown in Figure 5(p), DSS + SIN mice exhibited a a greater presence of *g-Rikenella* (marked in the orange box) and *g-UBA1819* (marked in the blue box), compared to those induced with DSS alone. We suspected *g-Rikenella* might be the most important gut microbiota in the role of SIN in improving colitis.

PICRUSt was employed to forecast the roles of gut microbiota. According to KEGG functional enrichment annotation (Figure 5(q)), several predicted functional differences were observed among the three groups. Among them, the two pathways with the greatest differences are amino acid metabolism (Figure 5(r)) and carbohydrate metabolism (Figure 5(s)). Collectively, our findings suggest that the beneficial outcomes of SIN therapy depended on regulating intestinal microbiota.

3.6. SIN Regulated SCFAs in DSS-Induced Chronic Colitis Mice. SCFAs are one of the major metabolites of the gut microbiota, and their production rate varies depending on

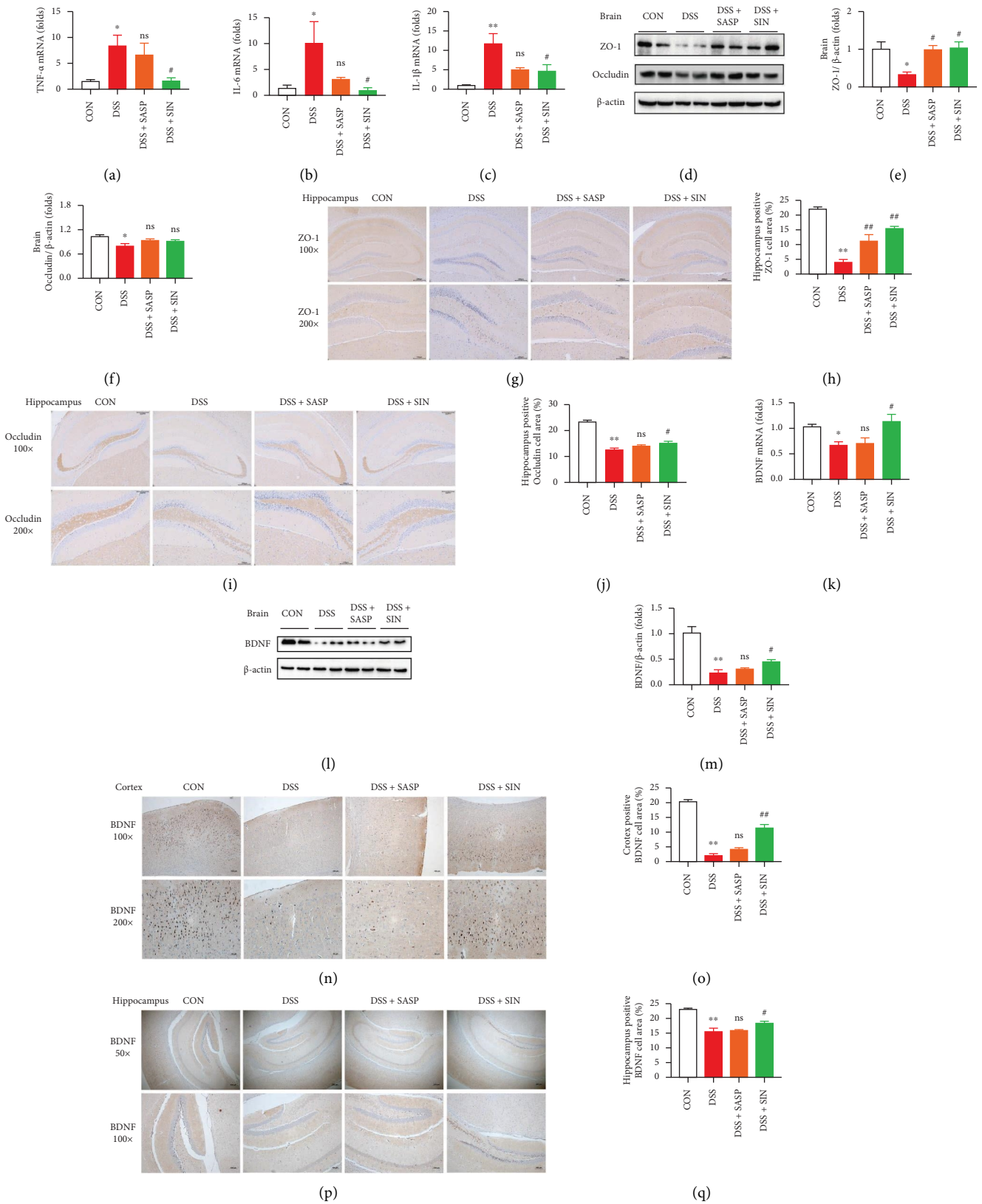


Figure 4: SIN protected against DSS-induced imbalance of neuroinflammation and ZO-1, BDNF expressions. The relative mRNA level of (a) TNF-α, (b) IL-6, and (c) IL-1β in the brain tissues. (d) Western blot analysis of ZO-1 and Occludin in the brain tissues. (e, f) Densitometry analysis of (d). Representative IHC micrographs of (g) ZO-1 and (i) Occludin protein in the hippocampus. (h) Statistical data of (G). (j) Statistical data of (i). (k) BDNF mRNA level expression in the brain tissues. (l) BDNF protein level expression in the brain tissues. (m) Densitometry analysis of (l). Representative IHC micrographs of BDNF protein in the (n) cortex and (p) hippocampus. (o) Statistical data of (n). (q) Statistical data of (p). Data are presented as the mean ± SEM, $n = 3$–6. $^{*}p < 0.05$ and $^{**}p < 0.01$ compared with CON, $^{\#}p < 0.05$ and $^{\#\#}p < 0.01$ compared with DSS, ns, no significant difference.

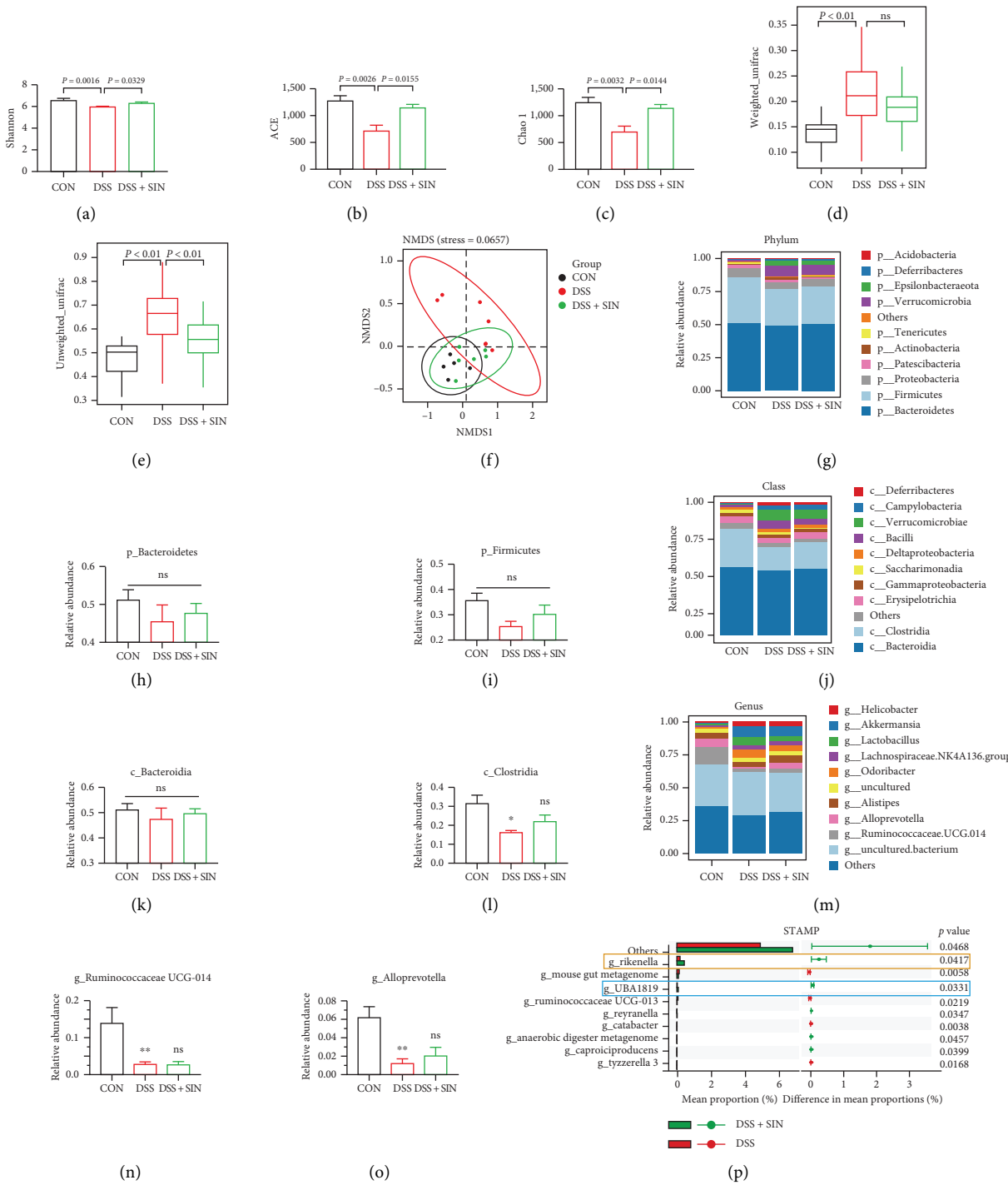
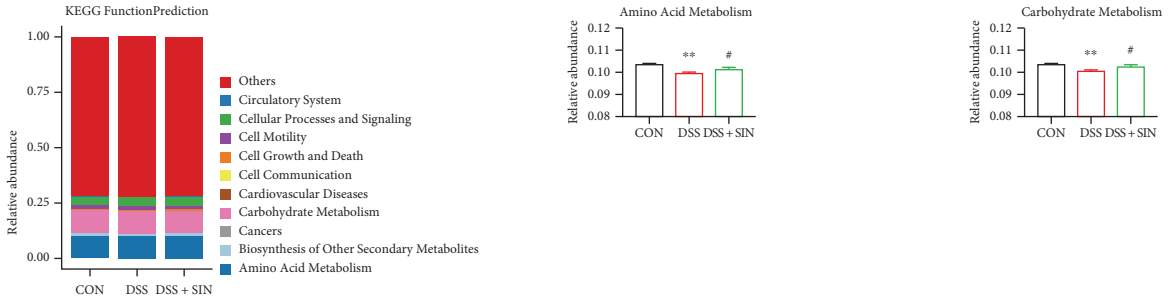


Figure 5: Continued.



(q) (r) (s)

FIGURE 5: SIN impacted the irregular gut microbiota composition in DSS-induced chronic colitis mice. (a) Shannon, (b) ACE, and (c) Chao 1 indices represent the distribution of fecal microbiota α-diversity. (d) Weighted Unifrac and (e) Unweighted Unifrac Beta distance showed the β-diversity. (f) Nonmetric multidimensional scaling (NMDS) revealed the bacterial community composition. Relative abundances of bacterial in (g) phylum, (j) class, and (m) genus levels. Relative abundances of (h) p-Bacteroidetes, (i) p-Firmicutes, (k) c-Bacteroidia, (l) c-Clostridia, (n) *g-Ruminococcaceae UCG-014*, and (o) *g-Alloprevotella*. (p) STAMP differential analysis between DSS + SIN and DSS at the genus level. (q) KEGG functional enrichment annotation. Relative abundance of (r) amino acid metabolism and (s) carbohydrate metabolism based on KEGG function prediction. Data are presented as the mean ± SEM, $n = 5–10$. $^{*}p < 0.05$ and $^{**}p < 0.01$ compared with CON, $^{\#}p < 0.05$ and $^{\#\#}p < 0.01$ compared with DSS, ns, no significant difference.

the composition of the gut bacteria [33, 34]. SCFAs are the typical metabolites of *Rikenella* [35]. *UBA1819* was also reported to be associated with enhanced butyrate production [36]. In addition, the SCFAs synthesis is mainly divided into two categories: (1) using dietary fiber as substrate through carbon metabolism; (2) using amino acids as substrates to synthesize branched SCFAs [37]. These results proved that SCFAs played a key role in SIN improving colitis.

Given that SIN relieved the accompanying memory disorder in DSS-induced chronic colitis. Circulating SCFAs have demonstrated positive effects on the metabolism and allied function of tissues and organs beyond the colon [38, 39]. We then determined the SCFAs content and composition in serum. The administration of DSS notably reduced the overall and individual SCFA levels (including acetic, propionic, butyric, and isobutyric acids) in the serum (Figures 6(a), 6(b),6(c), 6(d), 6(e)), along with a notable rise in the levels of hexanoic acid and valeric acid (Figures 6(f), 6(g)). Nevertheless, the DSS + SIN treatment significantly increased the levels of total SCFAs and specific SCFA components, such as acetic acid and isobutyric acid (Figures 6(a), 6(b), 6(e)), and reduced hexanoic acid (Figure 6(f)). There seemed no change in the serum isovaleric acid (Figure 6(h)).

SCFAs in feces were also detected. As shown in Figures 6(i), 6(k),6(l), 6(m), 6(n), 6(o), the total SCFA concentration and the contents of various types of SCFAs presented a significant decline in the DSS group than in the control group. Compared with those in the DSS group, the concentrations of total SCFAs, propionic acid, butyric acid, isobutyric acid, hexanoic acid, and valeric acid in the DSS + SIN group significantly increased. Compared to the CON group, DSS caused a significant rise of isovaleric acid, while DSS + SIN treatment caused a decline than the DSS group (Figure 6(p)). There seemed no statistical difference in the feces acetic acid (Figure 6(j)).

Furthermore, Spearman correlation analysis was performed at the genus level to investigate the relationships between altered gut microbiota and serum SCFAs after SIN intervention. As shown in Figure 6(q), the changes of SCFA in serum are closely related to the alterations of gut microbiota, especially acetic acid. Serum acetic acid was negatively related to *Ruminococcaceae UCG-013, Tyzzerella 3* and *Catabacter*, and positively associated with *Reyranella*, *anaerobic digester metagenome*, *UBA1819*, *Rikenella*, and *Caproiciproducens*. These results indicated that SIN regulates the serum and feces SCFA contents in DSS-induced chronic colitis mice. And SIN mitigated the accompanying memory disorder probability via gut microbiota–mediated SCFAs.

4. Discussion

The gut and brain are increasingly linked in human disease, and IBD displays an ever-expanding list of neurological comorbidities [40], including anxiety and depression [41, 42]. Growing evidences have shown that the DSS-induced colitis model in mice not only causes diarrhea and mucosal ulcers but also results in behavioral abnormalities [43, 44]. Compared with acute colitis, chronic experimental colitis in mice was induced by repeated exposure to DSS, with alternating periods of remission and relapse [45, 46], closely resembling human IBD symptoms [47, 48]. In addition, the advantages of the chronic models may offer better insight into complications [20, 49]. The severity of the colitis can be modulated by the dose and administration pattern of DSS, thus avoiding the possible risk of colorectal cancer caused by long-term DSS exposure. Based on these, the chronic colitis mice model was established with three cycles of 2.5%DSS in this article.

It was demonstrated that biological sex strongly influences colonic inflammation and exposure to chronic stress has a more pronounced effect in females than in males [50]. The adaptive immune cells, contacts, and CNs were

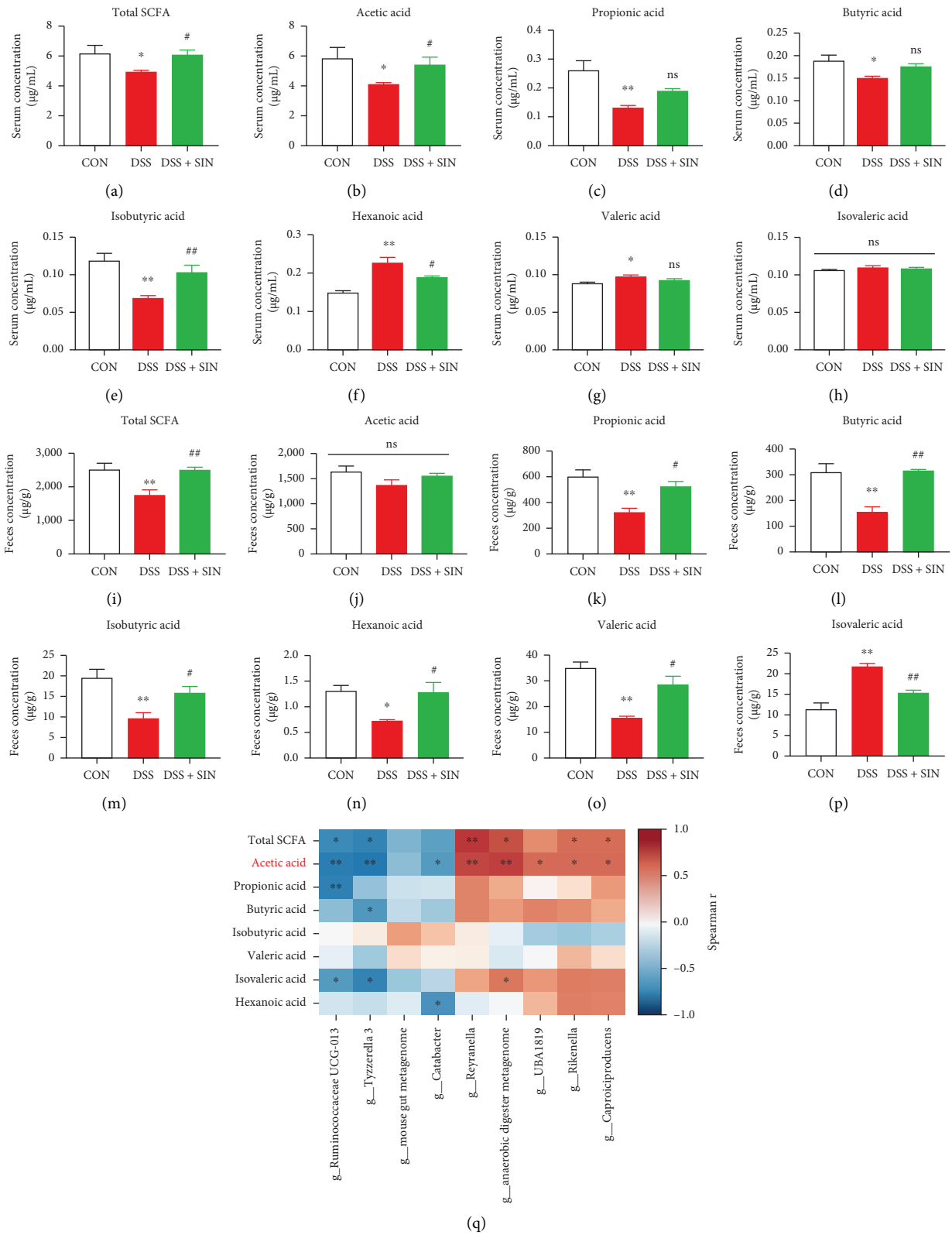


FIGURE 6: SIN regulated SCFAs in DSS-induced chronic colitis mice (a, i) Total SCFAs. (b, j) Acetic acids. (c, k) Propionic acids. (d, l) Butyric acids. (e, m) Isobutyric acids. (f, n) Hexanoic acid. (g, o) Valeric acid. (h, p) Isovaleric acid. Data are presented as the mean ± SEM, $n = 5–8$. $^{*}p < 0.05$ and $^{**}p < 0.01$ compared with CON, $^{\#}p < 0.05$ and $^{\#\#}p < 0.01$ compared with DSS, ns, no significant difference. (q) The relationship between serum SCFAs and the gut microbiota presented in Fig. 5p, using the Spearman correlation coefficient method. $^{*}p < 0.05$ and $^{**}p < 0.01$.

enriched in female patients compared to males [51]. Women with IBD tend to experience higher levels of depression, anxiety, and worse quality of life compared to men [52]. Here, we used female mice in all animal experiments, as they are commonly used in chemically induced intestinal inflammation in our lab, with robust and reproducible data.

Pharmacologically, SIN has been utilized to significantly inhibit inflammatory reactions safely since the 1920s [53–56]. Our previous studies showed that SIN could effectively alleviate DSS-induced acute UC [18]. In this study, the repeated administration of DSS effectively established a chronic colitis model in mice, as evidenced by phenotypic observations. Body weight loss and colonic shortening are closely related to the digestive and absorptive function, and systemic inflammatory responses [57]. In contrast to the DSS group, the DSS + SIN groups were able to mitigate weight loss, reduce the shortening of the colon, and lessen histopathological damage in the colon. SIN restored mice bodyweight that caused by DSS; this was perhaps because SIN could repress the inflammatory reaction of colon and repair colon barrier (Figure 3), which enhanced the digestion and absorption of intestine. In addition, our previous studies reported that SIN promoted 14-3-3θ protein expression and inhibited NF-κB p65 signaling in DSS-induced mice [17].

Functional MRI scans of patients in the active phase of UC revealed the reduced activity in the hippocampus and parahippocampus, which was linked to memory impairment [58]. It indicates that DSS-induced colitis influences stress-related behaviors and heightens anxiety and depression symptoms [43, 59], but the impact of a previous colitis episode on memory remains largely unexplored. In this study, mice were exposed to DSS-induced colitis for a duration of 5 days, and 5 days after stopping DSS intake, they underwent Pavlovian conditioned fear (CF) assessments. Contextual conditioning tests were employed to evaluate associative fear memory. Our results revealed that three rounds of DSS administration and intervals had no significant effect on short-term memory in mice. However, repeated DSS exposure significantly impairs long-term memory in mice, even in intervals. It illustrated that chronic colitis induced by DSS caused notable deficits in contextual fear memory, but only the DSS + SIN treatment was able to improve it in the third round over the long term (Figure 2(e), blue rectangle marked).

The hippocampus is a brain region critically involved in learning and memory processes [60]. Many researches indicate that neurons in the hippocampus encode contextual data and transmit it straight to the amygdala [61, 62]. Pathological changes in the hippocampal tissue of colitis mice were observed using Nissl staining and TUNEL staining. In DSS group, Nissl bodies exhibited deeper and denser, and hippocampal neurons showed apoptosis, indicative of pronounced cellular damage. However, DSS + SIN treatment significantly reduced them. It indicated that SIN protected hippocampal tissue, then improved the contextual memory function of hippocampus. Elevated levels of inflammatory cytokines in the gut can lead to dramatic effects outside the intestines. These cytokines can travel through the bloodstream and particularly disrupt the balance in the central nervous system (CNS) [8]. In this study, SIN obviously reduced the excessive inflammation in the colon and brain. It illustrated that SIN could effectively regulate the homeostasis of CNS. Inflammation in the intestines significantly also contributes to the breakdown of the mucosal barrier in the gut [63]. The absence of TJ proteins such as ZO-1 and Occludin is a crucial factor in the destruction of the intestinal mucosal barrier and the integrity of the BBB [64, 65]. Our results showed that SIN mitigated the reduction of ZO-1 and Occludin levels in the colon and also lessened the decline of ZO-1 expression in the brain. It further prompted that SIN protected the TJ proteins by suppressing inflammation in the colon and brain, then relieved the colonic and hippocampal injury. Our previous studies reported that SIN inhibited NF-κB p65 and Nrf2 signaling in the colon. The mechanism by which SIN ameliorates brain injury needs more deep studies.

BDNF is among the most extensively spread neurotrophins in the brains of mammals, playing a key role in the development of neurons and glial cells [66]. Human epidemiological evidence supports the role of BDNF in cognitive function and memory impairment. Improvements of memory and learning were accompanied by increased BDNF levels [31]. Our findings indicated that the DSS group mice exhibited reduced BDNF levels in the brain, while were mitigated by SIN treatment. It provides a promising development advantage of SIN in treating chronic colitis and accompanying memory disorders. Although the development of IBD is intricate, changes in the gut microbiome and metabolites, which are related in the intestinal mucosal barrier, extend an important impact in the communication of inflammatory signals via the gut–brain axis [67, 68]. Consequently, 16S rRNA sequencing was employed to examine the gut microbiota context and assess the impact of SIN intervention in mice. The findings indicated that SIN enhanced both the quantity and variety of gut microbiota in the experimental mice. Bacteroides and Firmicutes are common dominant bacterial groups in the gut, contributing to the organism's health by producing metabolites that support homeostasis and by competitively removing harmful pathogens [69]. Bacteroidia and Clostridia are classified as a class under the phylum Bacteroidetes and Firmicutes, respectively. Here, DSS + SIN treatment increased Bacteroides and Firmicutes compared with DSS group, indicating that SIN supplement could promote the increase of beneficial bacteria in the gut.

It is worth mentioning that SASP did not show neuroprotective in DSS-induced mice. After oral administration of SASP, a small part is absorbed in the gastrointestinal tract, and the unabsorbed part is broken down into 5-aminosalicylic acid (5-ASA) and sulfapyridine by bacteria in the terminal ileum and colon. 5-ASA is the active ingredient that ultimately works in colitis; it acts directly with inflammatory intestinal tissues and does not produce pharmacological effects through absorption. Sulfapyridine is a sulfonamide antibiotic. Both 5-ASA and sulfasalazine reduced the growth of healthy gut microbiota [70].

Moreover, STAMP analysis was conducted to explore the key gut microbiota at the genus level. *Rikenella* seems to play a vital role in the gut microbiome and may act as a probiotic, likely important for alleviating intestinal inflammation [35, 71]. Studies have shown that the levels of *Rikenella* in the intestines of individuals with IBD are markedly lower than those in healthy individuals [72, 73]. *Rikenella* aids in the formation of TJs in gut cells, promoting epithelial cell differentiation and enhancing the intestinal barrier [74, 75]. According to the reports, modifying the gut microbiota, such as *Rikenella*, through drug treatment enhanced intestinal permeability and reduced inflammation in mice [76]. Our results showed that SIN administration significantly increased the decline of *Rikenella* induced by DSS. It indicated that SIN reduced the inflammation and improved the barrier of colon by enhancing the proportion of *Rikenella* in the gut.

SCFAs, primarily generated by bacterial fermentation of dietary fiber in the digestive system, exhibit a crucial role in the communication among the microbiota, gut, and brain [77]. The majority of SCFAs are quickly absorbed from the intestinal cavity into the circulatory system, whereas less than 5% are eliminated through feces. SCFAs were absorbed by intestinal epithelial cells and are able to cross the blood–brain barriers via monocarboxylate transporters, thereby affecting CNS functions and altering cytokine levels [78, 79]. Hippocampal SCFA concentrations and receptor expressions were detected in the studies about intestinally derived SCFAs pass the blood–brain barrier through systemic circulation and take effect locally in the brain [80, 81]. Earlier research primarily examined SCFAs in the stool samples. Nonetheless, the suitability of using fecal SCFAs as an indicator for the host's SCFA levels remains uncertain. Our research involved quantifying SCFA concentrations in blood serum. Previous studies have shown that Firmicutes and Bacteroidetes are SCFAs producers [82]. *Rikenella* and *UBA1819* are also involved in SCFAs synthesis. *UBA1819*, from the Ruminococcaceae family, produce butyric acid via butyryl-CoA: acetate CoA-transferase with net consumption of acetic acid [83]. In this study, *Rikenella* and *UBA1819* showed a significant increase in the DSS + SIN group relative to the DSS group mice (Figure 5(p), marked in the orange and blue box). This may be one mechanism how SIN regulates SCFAs.

Accumulating data suggest that SCFAs have beneficial effects on regulation of brain function and BBB integrity, and SCFAs exert neuroprotective effects by upregulating glial-derived neurotrophic factors and BDNF [77, 84]. Here, we observed SIN supplement increased the total serum SCFAs and adjusted the imbalance of individual SCFA contents caused by DSS induction. Acetic acid, the most abundant SCFA, is primarily utilized by the liver for energy. It is capable of traversing the BBB, supplying energy to astrocytes, and then plays an important role in astrocyte-mediated immune functions within the brain [85]. Additionally, acetate enables metabolic fitness and cognitive performance [86]. Hepatic acetyl-CoA metabolism modulates neuro-inflammation and depression susceptibility via acetate [87]. We found that SIN supplement significantly reversed the decline of serum acetic acid level induced by DSS treatment. It indicated that SIN mitigated the accompanying memory disorder probability via SCFAs, especially acetic acid. Subsequent spearman correlation analysis showed that serum acetic acid had the closest correlation with gut microbiota between DSS and DSS + SIN groups. These above results highlight the neuroprotective function of SIN by regulating the SCFAs-producing gut microbiome and circulating SCFAs during DSS-induced chronic colitis. In addition, SCFAs may have additional regulatory effects on the production of neurotrophic factors. For instance, increased serum acetic acid can induce the elevations in hippocampal BDNF [88]. SIN also improved the BDNF expression in the brain. In this study, we speculated that SCFAs may be the key mediators in SIN that function through microbiota–gut–brain interactions.

5. Conclusion

In summary, from the perspective of memory disorder symptoms of chronic colitis, our results confirmed that SIN alleviates both DSS-induced chronic colitis and associated memory impairment by regulating gut homeostasis. The protective mechanism was linked to suppress colon inflammatory and repair colon barrier of UC mice. At the same time, SIN inhibited brain inflammation and hippocampal injury, promoted BBB repair, and increased the expression of BDNF. Furthermore, SIN regulated the gut microbiota and mediated SCFAs. These findings have significant implications for the development of novel therapeutic strategies for the treatment of both colitis and associated memory impairment. Most importantly, our study is of great significance for expanding the applications of SIN and exploring probiotics with treating memory disorder potential.

Nomenclature

SIN	Sinomenine
IBD	Inflammatory bowel diseases
BBB	Blood-brain barrier
NBF	Neutral buffered formalin
HE	Hematoxylin and eosin
TUNEL	TdT-mediated dUTP nick end labeling
SCFAs	Short-chain fatty acids
TJ	Tight junction
IL-1β	Interleukin-1 beta
IL-6	Interleukin-6
TNF-α	Tumor necrosis factor-α
BDNF	Brain-derived neurotrophic factor
CF	Conditioned fear
CNS	Central nervous system

Data Availability Statement

The data that support the findings of this study are available from the corresponding author upon reasonable request.

Conflicts of Interest

The authors declare no conflicts of interest.

Author Contributions

Yan Zhou contributed to writing–original draft, review and editing, methodology, formal analysis, conceptualization, and funding acquisition. Linxiao Wang contributed to methodology, software, data curation, and conceptualization. Jinjin Fu and Jie Zhao contributed to methodology. Dongmei Wang performed project administration. Liming Tang carried out funding acquisition. Yan Zhou and Linxiao Wang equally contributed to this manuscript.

Funding

This work was supported by grants from National Natural Science Foundation of China (grant number: 82273232), Natural Science Foundation of Jiangsu Province (grant number: BK20251772, BK20241775), Changzhou Sci&Tech Program (grant numbers: LC20252022CZLJ017, QY202306), Young Science & Technology Project of Changzhou Health Commission (grant number: QN202313, YJRC202408), and Changzhou Medical Center of Nanjing Medical University Program (grant number: CMCB202332, CMC2024PY01).

References

[1] J. S. Lasa, P. A. Olivera, S. Danese, and L. Peyrin-Biroulet, "Efficacy and Safety of Biologics and Small Molecule Drugs for Patients With Moderate-to-Severe Ulcerative Colitis: A Systematic Review and Network Meta-Analysis," *The lancet. Gastroenterology & hepatology* 7, no. 2 (2022): 161–170, https://doi.org/10.1016/s2468-1253(21)00377-0.

[2] M. Zhao, L. Gönczi, P. L. Lakatos, and J. Burisch, "The Burden of Inflammatory Bowel Disease in Europe in 2020," *Journal of Crohn's and Colitis* 15, no. 9 (2021): 1573–1587, https://doi.org/10.1093/ecco-jcc/jjab029.

[3] W. Wei, Y. Liu, Y. Hou, et al., "Psychological stress-induced Microbial Metabolite Indole-3-Acetate Disrupts Intestinal Cell Lineage Commitment," *Cell Metabolism* 36, no. 3 (2024): 466–483.e7, https://doi.org/10.1016/j.cmet.2023.12.026.

[4] B. Barberio, M. Zamani, C. J. Black, E. V. Savarino, and A. C. Ford, "Prevalence of Symptoms of Anxiety and Depression in Patients with Inflammatory Bowel Disease: a Systematic Review and Meta-Analysis," *The lancet. Gastroenterology & Hepatology* 6, no. 5 (2021): 359–370, https://doi.org/10.1016/s2468-1253(21)00014-5.

[5] A. D. Frolkis, I. A. Vallerand, A. A. Shaheen, et al., "Depression Increases the Risk of Inflammatory Bowel Disease, Which may be Mitigated by the Use of Antidepressants in the Treatment of Depression," *Gut* 68, no. 9 (2019): 1606–1612, https://doi.org/10.1136/gutjnl-2018-317182.

[6] S. Luo, Y. Chen, R. Zhao, et al., "Application of Omics Technology to Investigate the Mechanism Underlying the Role of San Hua Tang in Regulating Microglia Polarization and Blood-Brain Barrier Protection Following Ischemic Stroke," *Journal of Ethnopharmacology* 314 (2023): 116640, https://doi.org/10.1016/j.jep.2023.116640.

[7] Y. Wang, Q. Tan, M. Pan, et al., "Minimally Invasive Vagus Nerve Stimulation Modulates Mast Cell Degranulation via the microbiota-gut-brain Axis to Ameliorate Blood-Brain Barrier and Intestinal Barrier Damage Following Ischemic Stroke," *International Immunopharmacology* 132 (2024): 112030, https://doi.org/10.1016/j.intimp.2024.112030.

[8] G. Agirman, K. B. Yu, and E. Y. Hsiao, "Signaling Inflammation Across the Gut-Brain Axis," *Science (New York, N.Y.)* 374, no. 6571 (2021): 1087–1092, https://doi.org/10.1126/science.abi6087.

[9] A. Parker, S. Fonseca, and S. R. Carding, "Gut Microbes and Metabolites as Modulators of Blood-Brain Barrier Integrity and Brain Health," *Gut Microbes* 11, no. 2 (2020): 135–157, https://doi.org/10.1080/19490976.2019.1638722.

[10] Y. Y. Huang, Y. P. Wu, X. Z. Jia, et al., "*Lactiplantibacillus plantarum* DMDL 9010 Alleviates Dextran Sodium Sulfate (DSS)-Induced Colitis and Behavioral Disorders by Facilitating microbiota-Gut-Brain Axis Balance," *Food & Function* 13, no. 1 (2022): 411–424, https://doi.org/10.1039/d1fo02938j.

[11] M. Iacucci, G. Santacroce, S. Majumder, et al., "Opening the Doors of Precision Medicine: Novel Tools to Assess Intestinal Barrier in Inflammatory Bowel Disease and colitis-associated Neoplasia," *Gut* 73, no. 10 (2024): 1749–1762, https://doi.org/10.1136/gutjnl-2023-331579.

[12] X. Guo, J. Ji, Z. Feng, X. Hou, Y. Luo, and Z. Mei, "A Network Pharmacology Approach to Explore the Potential Targets Underlying the Effect of Sinomenine on Rheumatoid Arthritis," *International Immunopharmacology* 80 (2020): 106201, https://doi.org/10.1016/j.intimp.2020.106201.

[13] J. Yu, S. Wang, S. J. Chen, et al., "Sinomenine Ameliorates Fibroblast-like Synoviocytes Dysfunction by Promoting Phosphorylation and Nuclear Translocation of CRMP2," *Journal of Ethnopharmacology* 324 (2024): 117704, https://doi.org/10.1016/j.jep.2024.117704.

[14] S. Wang, L. Zhang, Y. Zhou, Z. Liu, Z. Zhou, and J. Huang, "A Review on Pharmacokinetics of Sinomenine and Its Anti-inflammatory and Immunomodulatory Effects," *International Immunopharmacology* 119 (2023): 110227, https://doi.org/10.1016/j.intimp.2023.110227.

[15] L. Huang, Y. Dong, J. Wu, et al., "Sinomenine-Induced Histamine Release-like Anaphylactoid Reactions Are Blocked by Tranilast via Inhibiting NF-κB Signaling," *Pharmacological Research* 125 (2017): 150–160, https://doi.org/10.1016/j.phrs.2017.08.014.

[16] Z. Shu, Y. Cao, Y. Tao, et al., "Polyvinylpyrrolidone Microneedles for Localized Delivery of Sinomenine Hydrochloride: Preparation, Release Behavior of in Vitro & in Vivo, and Penetration Mechanism," *Drug Delivery* 27, no. 1 (2020): 642–651, https://doi.org/10.1080/10717544.2020.1754524.

[17] Y. Zhou, S. Chen, Y. Dai, et al., "Sinomenine Attenuated Dextran Sulfate sodium-induced Inflammatory Responses by Promoting 14-3-3θ Protein and Inhibiting NF-κB Signaling," *Journal of Ethnopharmacology* 303 (2023): 116037, https://doi.org/10.1016/j.jep.2022.116037.

[18] Y. Zhou, S. Chen, W. Gu, X. Sun, L. Wang, and L. Tang, "Sinomenine Hydrochloride Ameliorates Dextran Sulfate Sodium-Induced Colitis in Mice by Modulating the Gut Microbiota Composition Whilst Suppressing the Activation of the NLRP3 Inflammasome," *Experimental and Therapeutic Medicine* 22, no. 5 (2021): 1287, https://doi.org/10.3892/etm.2021.10722.

[19] S. Louhimies, "Directive 86/609/EEC on the Protection of Animals Used for Experimental and Other Scientific Purposes," *Alternatives to Laboratory Animals* 30, no. 2_suppl (2002): 217–219, https://doi.org/10.1177/026119290203002s36.

[20] C. Yang and D. Merlin, "Unveiling Colitis: a Journey Through the Dextran Sodium Sulfate-Induced Model," *Inflammatory Bowel Diseases* 30, no. 5 (2024): 844–853, https://doi.org/10.1093/ibd/izad312.

[21] M. Mähler, I. J. Bristol, E. H. Leiter, et al., "Differential Susceptibility of Inbred Mouse Strains to Dextran Sulfate Sodium-Induced Colitis," *American Journal of Physiology Gastrointestinal and Liver Physiology* 274, no. 3 (1998): G544–G551, https://doi.org/10.1152/ajpgi.1998.274.3.g544.

[22] K. J. Livak and T. D. Schmittgen, "Analysis of Relative Gene Expression Data Using Real-Time Quantitative PCR and the 2−ΔΔCT Method," *Methods* 25, no. 4 (2001): 402–408, https://doi.org/10.1006/meth.2001.1262.

[23] H. Wang, S. Li, Z. Cui, et al., "Analysis of Spleen Histopathology, Splenocyte Composition and Haematological Parameters in Four Strains of Mice Infected with Plasmodium berghei K173," *Malaria Journal* 20, no. 1 (2021): 249, https://doi.org/10.1186/s12936-021-03786-z.

[24] Q. Su, J. Li, Y. Lu, et al., "Spleen Volume in Relation to Ulcerative Colitis and Crohn's Disease: a Mendelian Randomization Study," *Scientific Reports* 15, no. 1 (2025): 6588, https://doi.org/10.1038/s41598-025-90104-1.

[25] Y. Lei, M. Li, X. Liu, L. Zhang, R. Zhang, and F. Cai, "Nerolidol Rescues Hippocampal Injury of Diabetic Rats Through Inhibiting NLRP3 Inflammasome and Regulation of MAPK/AKT Pathway," *BioFactors* 50, no. 6 (2024): 1076–1100, https://doi.org/10.1002/biof.2058.

[26] S. Dai, J. Wei, H. Zhang, et al., "Intermittent Fasting Reduces Neuroinflammation in Intracerebral Hemorrhage Through the Sirt3/Nrf2/HO-1 Pathway," *Journal of Neuroinflammation* 19, no. 1 (2022): 122, https://doi.org/10.1186/s12974-022-02474-2.

[27] J. Machado Batista Sohn, N. C. Cardoso, A. M. Raymundi, J. Prickaerts, and C. A. J. Stern, "Phosphodiesterase 4 Inhibition After Retrieval Switches the Memory Fate Favoring Extinction Instead of Reconsolidation," *Scientific Reports* 13, no. 1 (2023): 20384, https://doi.org/10.1038/s41598-023-47717-1.

[28] X. Bao, Y. Tang, Y. Lv, et al., "Tetrastigma hemsleyanum Polysaccharide Ameliorated Ulcerative Colitis by Remodeling Intestinal Mucosal Barrier Function via Regulating the SOCS1/JAK2/STAT3 Pathway," *International Immunopharmacology* 137 (2024): 112404, https://doi.org/10.1016/j.intimp.2024.112404.

[29] I. Galea, "The Blood-Brain Barrier in Systemic Infection and Inflammation," *Cellular and Molecular Immunology* 18, no. 11 (2021): 2489–2501, https://doi.org/10.1038/s41423-021-00757-x.

[30] A. X. Gao, T. C. Xia, L. S. Lin, T. T. Dong, and K. W. Tsim, "The Neurotrophic Activities of Brain-Derived Neurotrophic Factor Are Potentiated by Binding with Apigenin, a Common Flavone in Vegetables, in Stimulating the Receptor Signaling," *CNS Neuroscience and Therapeutics* 29, no. 10 (2023): 2787–2799, https://doi.org/10.1111/cns.14230.

[31] K. Seidler and M. Barrow, "Intermittent Fasting and Cognitive Performance Targeting BDNF as Potential Strategy to Optimise Brain Health," *Frontiers in Neuroendocrinology* 65 (2022): 100971, https://doi.org/10.1016/j.yfrne.2021.100971.

[32] A. Lavelle and H. Sokol, "Gut microbiota-derived Metabolites as Key Actors in Inflammatory Bowel Disease," *Nature Reviews Gastroenterology & Hepatology* 17, no. 4 (2020): 223–237, https://doi.org/10.1038/s41575-019-0258-z.

[33] S. Sanna, N. R. van Zuydam, A. Mahajan, et al., "Causal Relationships Among the Gut Microbiome, Short-Chain Fatty Acids and Metabolic Diseases," *Nature Genetics* 51, no. 4 (2019): 600–605, https://doi.org/10.1038/s41588-019-0350-x.

[34] N. T. Baxter, A. W. Schmidt, A. Venkataraman, K. S. Kim, C. Waldron, and T. M. Schmidt, "Dynamics of Human Gut Microbiota and Short-Chain Fatty Acids in Response to Dietary Interventions With Three Fermentable Fibers," *mBio* 10, no. 1 (2019): e02566-18, https://doi.org/10.1128/mbio.02566-18.

[35] L. M. Cox, S. Yamanishi, J. Sohn, et al., "Altering the Intestinal Microbiota During a Critical Developmental Window has Lasting Metabolic Consequences," *Cell* 158, no. 4 (2014): 705–721, https://doi.org/10.1016/j.cell.2014.05.052.

[36] Y. H. Lee, P. Kalailingam, J. A. Delcour, V. Fogliano, and T. Thanabalu, "Olive-Derived Antioxidant Dietary Fiber Modulates Gut Microbiota Composition and Attenuates Atopic Dermatitis like Inflammation in Mice," *Molecular Nutrition & Food Research* 67, no. 10 (2023): e2200127, https://doi.org/10.1002/mnfr.202200127.

[37] C. Martin-Gallausiaux, L. Marinelli, H. M. Blottière, P. Larraufie, and N. Lapaque, "SCFA: Mechanisms and Functional Importance in the Gut," *Proceedings of the Nutrition Society* 80 (2021): 37–49.

[38] B. van der Hee and J. M. Wells, "Microbial Regulation of Host Physiology by Short-Chain Fatty Acids," *Trends in Microbiology* 29, no. 8 (2021): 700–712, https://doi.org/10.1016/j.tim.2021.02.001.

[39] Y. P. Silva, A. Bernardi, and R. L. Frozza, "The Role of Short-Chain Fatty Acids From Gut Microbiota in Gut-Brain Communication," *Frontiers in Endocrinology* 11 (2020): 25, https://doi.org/10.3389/fendo.2020.00025.

[40] J. S. Boles, M. E. Krueger, J. E. Jernigan, et al., "A Leaky Gut Dysregulates Gene Networks in the Brain Associated With Immune Activation, Oxidative Stress, and Myelination in a Mouse Model of Colitis," *Brain, Behavior, and Immunity* 117 (2024): 473–492, https://doi.org/10.1016/j.bbi.2024.02.007.

[41] S. C. Ng, H. Y. Shi, N. Hamidi, et al., "Worldwide Incidence and Prevalence of Inflammatory Bowel Disease in the 21st Century: a Systematic Review of Population-Based Studies," *The Lancet* 390, no. 10114 (2017): 2769–2778, https://doi.org/10.1016/s0140-6736(17)32448-0.

[42] A. Mikocka-Walus, S. R. Knowles, L. Keefer, and L. Graff, "Controversies Revisited:Aa Systematic Review of the Comorbidity of Depression and Anxiety With Inflammatory Bowel Diseases," *Inflammatory Bowel Diseases* 22, no. 3 (2016): 752–762, https://doi.org/10.1097/mib.0000000000000620.

[43] X. Chen, H. Zhao, Y. Lu, F. Meng, Z. Lu, and Y. Lu, "Surfactin Mitigates Dextran Sodium Sulfate-Induced Colitis and Behavioral Disorders in Mice by Mediating gut-brain-axis Balance," *Journal of Agricultural and Food Chemistry* 71, no. 3 (2023): 1577–1592, https://doi.org/10.1021/acs.jafc.2c07369.

[44] Z. J. Wang, L. H. Chen, J. Xu, Q. X. Xu, W. Xu, and X. W. Yang, "Corylin Ameliorates Chronic Ulcerative Colitis via Regulating the Gut-Brain Axis and Promoting 5-hydroxytryptophan Production in the Colon," *Phytomedicine* 110 (2023): 154651, https://doi.org/10.1016/j.phymed.2023.154651.

[45] H. L. Mok, K. W. Cheng, Y. Xu, et al., "Modified Zhenwu Decoction Suppresses Chronic Colitis via Targeting Macrophage CCR2/Fyn/p38 MAPK Signaling Axis," *Phytomedicine* 129 (2024): 155694, https://doi.org/10.1016/j.phymed.2024.155694.

[46] I. A. Gampierakis, Y. Koutmani, M. Semitekolou, et al., "Hippocampal Neural Stem Cells and Microglia Response to Experimental Inflammatory Bowel Disease (IBD)," *Molecular Psychiatry* 26, no. 4 (2021): 1248–1263, https://doi.org/10.1038/s41380-020-0651-6.

[47] H. M. Xu, H. L. Huang, Y. D. Liu, et al., "Selection Strategy of Dextran Sulfate Sodium-Induced Acute or Chronic Colitis

Mouse Models Based on Gut Microbial Profile," *BMC Microbiology* 21, no. 1 (2021): 279, https://doi.org/10.1186/s12866-021-02342-8.

[48] Y. Wang, L. Li, S. Chen, et al., "Faecalibacterium prausnitzii-derived Extracellular Vesicles Alleviate Chronic colitis-related Intestinal Fibrosis by Macrophage Metabolic Reprogramming," *Pharmacological Research* 206 (2024): 107277, https://doi.org/10.1016/j.phrs.2024.107277.

[49] S. Wirtz, V. Popp, M. Kindermann, et al., "Chemically Induced Mouse Models of Acute and Chronic Intestinal Inflammation," *Nature Protocols* 12, no. 7 (2017): 1295–1309, https://doi.org/10.1038/nprot.2017.044.

[50] R. M. Maltz, P. Marte-Ortiz, M. G. McClinchie, M. E. Hilt, and M. T. Bailey, "T Cell-Induced Colitis Is Exacerbated by Prolonged Stress: a Comparison in Male and Female Mice," *Biomedicines* 12, no. 1 (2024): 214, https://doi.org/10.3390/biomedicines12010214.

[51] A. T. Mayer, D. R. Holman, A. Sood, et al., "A Tissue Atlas of Ulcerative Colitis Revealing Evidence of Sex-Dependent Differences in Disease-riving Inflammatory Cell Types and Resistance to TNF Inhibitor Therapy," *Science Advances* 9, no. 3 (2023): eadd1166, https://doi.org/10.1126/sciadv.add1166.

[52] S. Pace, K. P. L. Meyer, F. Troisi, et al., "Sex Hormone Deprivation Abolishes Sex-specific Differences in Murine Colon Inflammation and Related Lipid Mediator Production," *The FASEB Journal* 38, no. 14 (2024): e23828, https://doi.org/10.1096/fj.202400320r.

[53] K. Chan, Z. Q. Liu, Z. H. Jiang, et al., "The Effects of Sinomenine on Intestinal Absorption of Paeoniflorin by the Everted Rat Gut Sac Model," *Journal of Ethnopharmacology* 103, no. 3 (2006): 425–432, https://doi.org/10.1016/j.jep.2005.08.020.

[54] Y. Lin, Y. Tang, O. Yi, et al., "Graphene Oxide Quantum dots-loaded Sinomenine Hydrochloride Nanocomplexes for Effective Treatment of Rheumatoid Arthritis via Inducing Macrophage Repolarization and Arresting Abnormal Proliferation of Fibroblast-like Synoviocytes," *Journal of Nanobiotechnology* 22, no. 1 (2024): 383, https://doi.org/10.1186/s12951-024-02645-8.

[55] Q. Yang, Q. Chen, K. B. Zhang, et al., "Sinomenine Alleviates Neuroinflammation in Chronic Cerebral Hypoperfusion by Promoting M2 Microglial Polarization and Inhibiting Neuronal Pyroptosis via Exosomal miRNA-223-3p," *Acta neuropathologica communications* 13, no. 1 (2025): 48, https://doi.org/10.1186/s40478-025-01950-z.

[56] W. Y. Guo, Q. M. Wu, H. F. Zeng, et al., "A Sinomenine Derivative Alleviates Bone Destruction in Collagen-Induced Arthritis Mice by Suppressing Mitochondrial Dysfunction and Oxidative Stress via the NRF2/HO-1/NQO1 Signaling Pathway," *Pharmacological Research* 215 (2025): 107686, https://doi.org/10.1016/j.phrs.2025.107686.

[57] C. Liu, H. Hua, H. Zhu, et al., "Aloe Polysaccharides Ameliorate Acute Colitis in Mice via Nrf2/HO-1 Signaling Pathway and Short-Chain Fatty Acids Metabolism," *International Journal of Biological Macromolecules* 185 (2021): 804–812, https://doi.org/10.1016/j.ijbiomac.2021.07.007.

[58] W. Fan, S. Zhang, J. Hu, et al., "Aberrant Brain Function in Active-Stage Ulcerative Colitis Patients: A Resting-State Functional MRI Study," *Frontiers in Human Neuroscience* 13 (2019): 107, https://doi.org/10.3389/fnhum.2019.00107.

[59] H. Liu, J. Sun, Z. Wang, et al., "S100a10 Deficiency in Neutrophils Aggravates Ulcerative Colitis in Mice," *International Immunopharmacology* 128 (2024): 111499, https://doi.org/10.1016/j.intimp.2024.111499.

[60] X. Fu, S. Yan, Z. Hu, et al., "Guhan Yangsheng Jing Mitigates Hippocampal Neuronal Pyroptotic Injury and Manifies Learning and Memory Capabilities in Sleep Deprived Mice via the NLRP3/Caspase1/GSDMD Signaling Pathway," *Journal of Ethnopharmacology* 326 (2024): 117972, https://doi.org/10.1016/j.jep.2024.117972.

[61] C. Xu, S. Krabbe, J. Gründemann, et al., "Distinct Hippocampal Pathways Mediate Dissociable Roles of Context in Memory Retrieval," *Cell* 167, no. 4 (2016): 961–972.e16, https://doi.org/10.1016/j.cell.2016.09.051.

[62] W. B. Kim and J. H. Cho, "Encoding of Contextual Fear Memory in Hippocampal-Amygdala Circuit," *Nature Communications* 11, no. 1 (2020): 1382, https://doi.org/10.1038/s41467-020-15121-2.

[63] X. Li, Q. Li, B. Xiong, H. Chen, X. Wang, and D. Zhang, "Discoidin Domain Receptor 1(DDR1) Promote Intestinal Barrier Disruption in Ulcerative Colitis Through Tight Junction Proteins Degradation and Epithelium Apoptosis," *Pharmacological Research* 183 (2022): 106368, https://doi.org/10.1016/j.phrs.2022.106368.

[64] L. Cui, X. Guan, W. Ding, et al., "Scutellaria baicalensis Georgi Polysaccharide Ameliorates DSS-Induced Ulcerative Colitis by Improving Intestinal Barrier Function and Modulating Gut Microbiota," *International Journal of Biological Macromolecules* 166 (2021): 1035–1045, https://doi.org/10.1016/j.ijbiomac.2020.10.259.

[65] Y. Liu, L. Wang, N. Du, X. Yin, H. Shao, and L. Yang, "Ramelteon Ameliorates LPS-Induced Hyperpermeability of the Blood-Brain Barrier (BBB) by Activating Nrf2," *Inflammation* 44, no. 5 (2021): 1750–1761, https://doi.org/10.1007/s10753-021-01451-w.

[66] P. Kowiański, G. Lietzau, E. Czuba, M. Waśkow, A. Steliga, and J. Moryś, "BDNF: a Key Factor With Multipotent Impact on Brain Signaling and Synaptic Plasticity," *Cellular and Molecular Neurobiology* 38, no. 3 (2018): 579–593, https://doi.org/10.1007/s10571-017-0510-4.

[67] J. Hu, H. Huang, Y. Che, et al., "Qingchang Huashi Formula Attenuates DSS-Induced Colitis in Mice by Restoring Gut Microbiota-Metabolism Homeostasis and Goblet Cell Function," *Journal of Ethnopharmacology* 266 (2021): 113394, https://doi.org/10.1016/j.jep.2020.113394.

[68] I. Grosheva, D. Zheng, M. Levy, et al., "High-Throughput Screen Identifies Host and Microbiota Regulators of Intestinal Barrier Function," *Gastroenterology* 159, no. 5 (2020): 1807–1823, https://doi.org/10.1053/j.gastro.2020.07.003.

[69] A. L. Komaroff, "The Microbiome and Risk for Obesity and Diabetes," *JAMA* 317, no. 4 (2017): 355–356, https://doi.org/10.1001/jama.2016.20099.

[70] L. E. McCoubrey, N. Seegobin, N. Sangfuang, et al., "The Colon Targeting Efficacies of Mesalazine Medications and Their Impacts on the Gut Microbiome," *Journal of Controlled Release* 369 (2024): 630–641, https://doi.org/10.1016/j.jconrel.2024.04.016.

[71] Y. Liao, Z. Peng, L. Chen, A. K. Nüssler, L. Liu, and W. Yang, "Deoxynivalenol, Gut Microbiota and Immunotoxicity: A Potential Approach?" *Food and Chemical Toxicology* 112 (2018): 342–354, https://doi.org/10.1016/j.fct.2018.01.013.

[72] L. R. Lopetuso, V. Petito, C. Graziani, et al., "Gut Microbiota in Health, Diverticular Disease, Irritable Bowel Syndrome, and Inflammatory Bowel Diseases: Time for Microbial Marker of Gastrointestinal Disorders," *Digestive Diseases* 36, no. 1 (2018): 56–65, https://doi.org/10.1159/000477205.

[73] X. C. Morgan, T. L. Tickle, H. Sokol, et al., "Dysfunction of the Intestinal Microbiome in Inflammatory Bowel Disease and Treatment," *Genome Biology* 13, no. 9 (2012): R79, https://doi.org/10.1186/gb-2012-13-9-r79.

[74] P. D. Cani, S. Possemiers, T. Van de Wiele, et al., "Changes in Gut Microbiota Control Inflammation in Obese Mice Through a Mechanism Involving GLP-2-driven Improvement of Gut Permeability," *Gut* 58, no. 8 (2009): 1091–1103, https://doi.org/10.1136/gut.2008.165886.

[75] X. Zhang, Y. Zhao, M. Zhang, et al., "Structural Changes of Gut Microbiota During Berberine-Mediated Prevention of Obesity and Insulin Resistance in High-Fat Diet-Fed Rats," *PLoS One* 7, no. 8 (2012): e42529, https://doi.org/10.1371/journal.pone.0042529.

[76] T. T. Cai, X. L. Ye, R. R. Li, et al., "Resveratrol Modulates the Gut Microbiota and Inflammation to Protect Against Diabetic Nephropathy in Mice," *Frontiers in Pharmacology* 11 (2020): 1249, https://doi.org/10.3389/fphar.2020.01249.

[77] B. Dalile, L. Van Oudenhove, B. Vervliet, and K. Verbeke, "The Role of Short-Chain Fatty Acids in Microbiota-Gut-Brain Communication," *Nature Reviews Gastroenterology & Hepatology* 16, no. 8 (2019): 461–478, https://doi.org/10.1038/s41575-019-0157-3.

[78] S. Ju, Y. Shin, S. Han, et al., "The Gut-Brain Axis in Schizophrenia: the Implications of the Gut Microbiome and SCFA Production," *Nutrients* 15, no. 20 (2023): 4391, https://doi.org/10.3390/nu15204391.

[79] R. W. Mitchell, N. H. On, M. R. Del Bigio, D. W. Miller, and G. M. Hatch, "Fatty Acid Transport Protein Expression in Human Brain and Potential Role in Fatty Acid Transport Across Human Brain Microvessel Endothelial Cells," *Journal of Neurochemistry* 117, no. 4 (2011): 735–746, https://doi.org/10.1111/j.1471-4159.2011.07245.x.

[80] W. Xiao, J. Su, X. Gao, et al., "Correction to: The Microbiota-Gut-Brain Axis Participates in Chronic Cerebral Hypoperfusion by Disrupting the Metabolism of Short-Chain Fatty Acids," *Microbiome* 10, no. 1 (2022): 70, https://doi.org/10.1186/s40168-022-01277-0.

[81] Y. Sun, H. Zhang, X. Zhang, et al., "Promotion of Astrocyte-Neuron Glutamate-Glutamine Shuttle by SCFA Contributes to the Alleviation of Alzheimer's Disease," *Redox Biology* 62 (2023): 102690, https://doi.org/10.1016/j.redox.2023.102690.

[82] J. Rodriguez, S. Hiel, A. M. Neyrinck, et al., "Discovery of the Gut Microbial Signature Driving the Efficacy of Prebiotic Intervention in Obese Patients," *Gut* 69, no. 11 (2020): 1975–1987, https://doi.org/10.1136/gutjnl-2019-319726.

[83] R. Salvado, S. Santos-Minguez, C. Lugones-Sánchez, et al., "Gut Microbiota and Its Relationship With Early Vascular Ageing in a Spanish Population (MIVAS Study)," *European Journal of Clinical Investigation* 54, no. 9 (2024): e14228, https://doi.org/10.1111/eci.14228.

[84] L. Hoyles, T. Snelling, U. K. Umlai, et al., "Microbiome-Host Systems Interactions: Protective Effects of Propionate Upon the Blood-Brain Barrier," *Microbiome* 6, no. 1 (2018): 55, https://doi.org/10.1186/s40168-018-0439-y.

[85] M. A. González Hernández, E. E. Canfora, J. W. E. Jocken, and E. E. Blaak, "The Short-Chain Fatty Acid Acetate in Body Weight Control and Insulin Sensitivity," *Nutrients* 11, no. 8 (2019): 1943, https://doi.org/10.3390/nu11081943.

[86] Q. He, L. Ji, Y. Wang, et al., "Acetate Enables Metabolic Fitness and Cognitive Performance During Sleep Disruption," *Cell Metabolism* 36, no. 9 (2024): 1998–2014.e15, https://doi.org/10.1016/j.cmet.2024.07.019.

[87] Y. Cao, Y. Zhao, T. Deng, et al., "Hepatic acetyl-CoA Metabolism Modulates Neuroinflammation and Depression Susceptibility via Acetate," *Cell Metabolism* 37, no. 11 (2025): 2185–2201.e8, https://doi.org/10.1016/j.cmet.2025.08.010.

[88] J. S. Church, J. A. M. Bannish, L. A. Adrian, K. Rojas Martinez, A. Henshaw, and J. J. Schwartzer, "Serum Short Chain Fatty Acids Mediate Hippocampal BDNF and Correlate with Decreasing Neuroinflammation Following High Pectin Fiber Diet in Mice," *Frontiers in Neuroscience* 17 (2023): 1134080, https://doi.org/10.3389/fnins.2023.1134080.